UNIVERSITY OF CALIFORNIA

SANTA CRUZ

Implementing State-dependent Models to Investigate Complex Life History Stages and Their Influence on Population Dynamics

A thesis submitted in partial satisfaction
of the requirements for the degree of

MASTER OF SCIENCE

in

STATISTICS AND APPLIED MATHEMATICS

by

Valerie Brown

Applied Mathematics and Statistics and Center for Stock Assessment Research

November 2011

The Thesis of Valerie Brown
is approved:

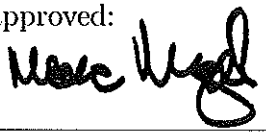

Professor Marc Mangel, Chair

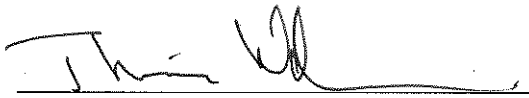

Thomas Williams

Abstract

Since data collection is expensive in terms of both money and time, few data sets are as complete as would be desired. Thus, through the use of modeling, scientists are able to expand their knowledge about a system. In particular, modeling is able to test multiple hypotheses regarding the underlying mechanisms producing the data. For three distinct topics, I address both management and biological problems through the use of modeling. Using a life history simulator, I test the assumptions made in a salmon stock assessment (cohort reconstruction). I find that the assessment method used tends to overestimate the abundance of the stock, and the assumed natural mortality function within the assessment plays an important role in this process. Additionally, I investigate the problem of forecasting fishing effort in a multiple well-mixed stock scenario (no single stock is targeted) through simulation. The model results demonstrate that combining information improves the forecasted effort estimate. Finally, using a state-dependent life history model, I investigate the optimal resource allocation for juvenile sea turtles in a toxic environment. The results indicate that the model is sensitive to the parameters values used, and as expected, smaller turtles must allocate more resources to growth (as opposed to detoxification) than larger turtles.

These models provide a framework for further investigations and similar problems. They also have the potential to influence the direction of future data collection.

Introduction

It is difficult to observe and collect data for many ecological processes. As technology improves and new scientific innovations are made, some questions can be answered, but many more remain, or are discovered as a product of the current work and results (Vicens and Bourne, 2007). Through the use of modeling, multiple approaches can be applied to a problem, and insights can be made into possible drivers of these phenomena. While data and results gained from field work are irreplaceable, this process is costly and filled with uncertainty. Modeling can help fill in gaps from missing data and attempt to give alternative explanations for observed data. I investigate three scientific problems through modeling.

The first problem I investigate provides a methodology for examining how well a model performs when the true dynamics of a population are more complex than the assumptions used to model that population. I use simulations to address this problem, and use Pacific salmon (*Oncorhynchus* spp.) for the model system. The next problem involves a parallel question more closely tied to management issues. I use simulation to help reconcile disparate harvest variables, which should agree across three stocks. The model system in this problem is again Pacific salmon. Finally, I consider what individual based models can tells us about resource allocation for juvenile sea turtles exposed to toxins. Given the current toxin load and weight of the individual, I use an optimization method to predict optimal resource allocation to detoxification or growth.

While each model is unique and addresses a separate biological and/or managerial issue, they all further our understanding of the model system and provide a framework for future investigation. Additionally, the results of these models illuminate issues in the tools used in management and where further investigation is necessary, as well as attempt to explain the mechanisms behind observed regional differences in physical and biochemical values. Each of these models has the potential to direct future data collection and thus better inform

research in these areas.

Chapter 1: A Life History Simulator to Test Stock Assessment Models and Methods

Introduction

Stock assessments are widely applied throughout fisheries management and are vital for evaluating the status and projecting the future catch of a stock (Gulland, 1988). In particular, stock assessments produce estimates of abundance, which fisheries managers use in establishing policies such as catch limits to prevent overfishing and maintain sustainable fisheries (Rose and Cowan, 2003). In order to perform a stock assessment, various relevant data for the stock, including both fisheries data (landings, coded wire tags, hatcheries) and fisheries independent data (egg/larval surveys), may be incorporated in the assessment. However, the inclusion of data that are not appropriate for the system being modeled can be detrimental to the accuracy of the results of the assessment; therefore only a subset of all available data may be used (Wang et al., 2009). The fisheries data may include the fishery type (commercial, recreational), total catch (biomass, numbers), geographic area of the catch, month and year of the catch, fishing effort, age composition of the catch, sex composition of the catch, and length or weight composition of the catch (Rose and Cowan, 2003; Chen et al., 2003). Alternatively, fisheries independent data may inform managers about the local movement and dispersal of the stock, migratory patterns, recapture rates, natural mortality estimates, growth rates, and other life history parameters (Gulland, 1988). Many stock assessments use these data as inputs to complex statistical analyses (e.g., Stock Synthesis 3 (SS3), details available at http://nft.nefsc.noaa.gov/SS3.html; the Ecosystem Diagnosis and Treatment (EDT) model discussed in McElhany et al., 2010; Chen et al., 2003). The results of this process determine the status of the stock and influence policies enacted regarding the stock (Figure 1).

Within a stock assessment assumptions must be made about the life history parameters and functional form of the population dynamics for the stock. These assumptions are traditionally drawn from data, borrowed from similar species, or come from convention (see Rose and Cowan, 2003 regarding estimates of steepness (the fraction of unfished recruitment expected when spawning biomass is at 20% of its unfished biomass), also see Mangel et al., 2010). For instance, accurately establishing the rate of natural mortality for a stock is quite difficult since this rate is not directly observable. Therefore, several equations estimating mortality have emerged including: constant mortality ($M = 0.2$), mortality depending on age ($M(a)$), and mortality depending on length at age ($M(L(a))$) (Jennings et al., 2001; Post and Evans, 1989; Lorenzen, 1996). Additionally, when using parametric models, the modeler must specify the recruitment relationship (functional form of the population dynamics); for instance, choosing between a Ricker recruitment model and a Beverton-Holt recruitment model (Ricker, 1958; Beverton and Holt, 1957). Although a range of parameters and functional forms governing the dynamics of the population may be used in the stock assessment, in order to make modeling the stock tractable, many scenarios must be excluded.

For example, consider the Namibian hake fishery (Hilborn and Mangel, 1997). An unregulated fishery developed on an unfished stock until a dramatic decrease in catch per unit effort (CPUE) was experienced. A regulatory agency was then established for the stock, leading to a reduction in catch. In order to model the fluctuating fish population dynamics, two models were considered, one less complex (4 free parameters) than the other (5 free parameters). Throughout the development of both the stochastic and deterministic models, Hilborn and Mangel (1997) made decisions regarding which parameters to derive from data, which parameters to specify a priori, and what types of uncertainty to include. After the models were developed and the CPUE data were input into both models, the authors determined which model best fit the data. "Best fit" was defined as the model that was the most consistent with the data and used the fewest free parameters. Hilborn and Mangel (1997)

found that for this data set the less "realistic" model (de Valpine and Hilborn, 2005) was a better fit (cf. Ludwig and Walters, 1985).

This process can become even more computationally intensive as more parameters and models are considered. Thus, investigating every possible scenario is not feasible; some assumptions must be made, no matter what type of model is used. This results in a disparity between assumptions made in the stock assessment tool and the true dynamics of the stock, which may have significant consequences for the output of the assessment. Through simulation, I propose to test the robustness of stock assessment tools to these assumptions. Similar to a Management Strategy Evaluation (MSE), I use an operating model that is more complex than the management tool to evaluate the management tool. However, while the focus of an MSE is to identify the most robust management procedure (including decision rules and management actions) across a variety of criteria, my work focuses on the assumptions within an assessment tool and the accuracy of population estimates derived from the assessment tool. Specifically, I simulate complex age structure for the species within the operating model, while the assessment tool does not take this complexity into account. Additionally, I investigate the importance of assuming a constant natural mortality rate within the assessment tool while the operating model is constructed with a non-constant natural mortality rate. This approach allows me to determine the type and quantity of error that emerges when the assumptions within the management tool differ from the true biology of the organism.

Different quantities and types of data are collected for different stocks (Chen et al., 2003). The variability in the data depends on the agency collecting the data and their jurisdiction, historical catch records, logistical limitations, funding and time constraints, the status of the stock, politics, and the importance of the stock both recreationally and commercially. A gradient in quality and quantity of data is expected across stocks that ranges from data poor to data rich (Figure 2). Data poor stocks are typically characterized by short time series

and include no records of catch composition, only total catch by numbers or biomass. Data rich stocks may be characterized by a long time series with diverse catch compositions such as catch by age, sex, length or weight, and location. Furthermore, data rich stocks may be described by data corresponding to movement, mortality and growth rates, effort, and other life history characteristics. Stocks that fall between the extremes of data poor and data rich are described by any subset of the data available for data rich stocks. Performing a stock assessment on a data poor stock adds another layer of complexity to the process since many of the life history parameters and assumptions about the dynamics of the stock must be determined without data (Wetzel and Punt, 2011). Even for data rich stocks, selecting the relevant data for the model can be quite challenging. Another goal of my research is to test the effectiveness of the stock assessment tool when confronted with various data levels. For example, I input a subset of the total catch time series into the assessment to determine the influence of the length of catch time series on the accuracy of the estimates generated by the assessment tool.

There are several sources of uncertainty in the stock assessment process: 1) the functional forms selected to model the dynamics of the stock, since there are often several appropriate functions available; 2) observation error due to the data collection method; 3) assumptions made about the available data, the system being examined, and the functions used during the modeling process, all incur additional uncertainty (Wang et al., 2009).

I develop a simulator, which I apply to the life history of Chinook salmon (*Oncorhynchus tshawytscha*). The simulator is parameterized for this species and details are discussed in the following sections. The simulator is constructed as a discrete time dynamical system that tracks the age (both river and ocean), length, and location of the population through time. The population size within a region changes as a result of mortality, recruitment and migration. The simulated stock generates catch and escapement data that are entered into a stock assessment model. The results from the assessment are compared to the full population

information to quantify stock assessment accuracy. This is peformed for both the full data set and a shortened data set to determine the change in accuracy under these two scenarios (Figure 3).

I describe the simulation model and identify the stock assessment that is tested with data generated from the simulation model. Finally, I present results for the accuracy of the stock assessment and end with a discussion (the work described here represents that done in Brown and Hively (2011)).

Simulation Model

Salmon stock assessments typically only model ocean abundance (Mohr, 2006b), but this simulator explicitly describes the egg, parr, at-sea, and spawner life history stages for salmon (Figure 4). The intermediate life stages that are not modeled (alevin, fry, smolt) can be subsumed into the following life history stage without the model losing biological relevance. For instance, the fry stage is not explicitly modeled. This life stage occurs between the egg and parr stage, thus it is collapsed into the parr stage. In this model, eggs transition into parr. Parr can remain in the river as parr or go (g) to the sea. The proportion of parr that remain in natal river i each time step is $1 - g(i)$, where there are a total of n rivers. The remaining proportion $g(i)$ of the parr transition to the at-sea stage. The at-sea fish can remain at-sea or return home (h) to spawn and produce eggs. These are modeled as proportions $1 - h(i)$ and $h(i)$, respectively. Table 1 contains a complete list of variables and their descriptions.

Individual Growth and Survival

To capture the dynamics of both river and ocean growth for salmon, I use a modified version of the standard von Bertalanffy growth equation, which describes the relationship between age (yr) and length (cm) with spatial variation via multiple rivers (von Bertalanffy, 1957). River growth alone, however, follows the standard von Bertalanffy growth equation.

This assumes that length is asymptotic for older ages, resulting in smaller increments to length as age increases. Additionally, I assume that growth can vary spatially (among rivers) within stocks (Boehlert and Kappenman, 1980; Haldorson and Love, 1990) due to variable amounts of resources and differing induced metabolic effects among regions. For a fish of river age a_r from natal river i with asymptotic size $L_\infty(i)$, an offset parameter $\tau_0(i)$ compensates for the initial size of an individual, and growth rate $k(i)$ determines how quickly individuals approach asymptotic size. The equation governing length at age in the river is

$$L_r(a_r, i) = L_\infty(i) \cdot \left(1 - e^{-k(i)\cdot\left(a_r - \tau_0(i)\right)}\right). \tag{1}$$

For a fish of ocean age a_o and river age a_r (e.g., age can be determined from scale samples) such that total age $a_T = a_r + a_o$, with growth rate k_o, asymptotic size $L_{o,\infty}$, and from natal river i, length at age in the ocean $L_o(a_r, a_o, i)$ is

$$L_o(a_r, a_o, i) = L_{o,\infty} \cdot \left(1 - e^{-k_o \cdot a_o}\right) + L_r(a_r, i) \cdot e^{-k_o \cdot a_o}. \tag{2}$$

Equation (2) has two distinct parts, the first term is the contribution to size from living in the ocean, given that the at-sea fish started at size $L_r(a_r, i)$, and the second term is the contribution to size from living in the river.

I assume an allometric relationship between length and weight $W(a_r, a_o, i)$ (gm), where c_1 denotes density and $c_2 \sim 3$ establishes an approximately cubic relationship between length and weight so that

$$W(a_r, a_o, i) = c_1 \cdot L_o(a_r, a_o, i)^{c_2}. \tag{3}$$

Total mortality $Z = M + \mathcal{F}$ (yr^{-1}) is determined by natural mortality M and fishing mortality $\mathcal{F}$. Larger size should decrease the types and number of predators able to consume individuals, and should allow larger stores of energy with which to resist disease or parasitism. These factors will vary by location since the habitat and ecosystem are spatially heterogeneous, resulting in differing sources of mortality across the seascape. I model the

size selectivity of mortality by including size-independent $M_{r,0}(a_r, i)$ (river) and $M_{o,0}(a_r, a_o, i)$ (ocean), and size-dependent $M_{r,1}(a_r, i)$ (river) and $M_{o,1}(a_r, a_o, i)$ (ocean) components that depend on river i. I represent natural mortality for river fish of age a_r in river i by $M_r(a_r, i)$:

$$M_r(a_r, i) = M_{r,0}(a_r, i) + \frac{M_{r,1}(a_r, i)}{L_r(a_r, i)}. \tag{4}$$

For ocean fish with river age a_r, ocean age a_o, from natal river i, the natural mortality rate $M_o(a_r, a_o, i)$ is described by

$$M_o(a_r, a_o, i) = M_{o,0}(a_r, a_o, i) + \frac{M_{o,1}(a_r, a_o, i)}{L_o(a_r, a_o, i)}. \tag{5}$$

The example assessment, described in a following section, is based on an assumption of constant natural mortality. I calculate five different values for the pair of parameters $(M_{o,0}(a_r, a_o, i)),\ M_{o,1}(a_r, a_o, i))$ associated with ocean natural mortality that generate the same survival to maximum age as constant mortality (dropping the region and age dependence for notation simplicity; see Appendix A for a description of the M_0 and M_1 parameter value calculations). I denote the five pairs as $M^* = \{M^*(1), M^*(2), M^*(3), M^*(4), M^*(5)\}$ where each j entry contains an (M_0, M_1) pair such that $M^*(j) = (M_0(j), M_1(j))$. These cases describe the proportion of natural mortality that is size-dependent, that is the proportion that is size-dependent for $M^*(1)$ is 0, so $M_1(1) = 0$ (corresponding to constant natural mortality), for $M^*(2)$ 25% of the total natural mortality is size-dependent, etc., up to $M^*(5)$ where 100% of the natural mortality is size-dependent so $M_0(5) = 0$. These cases are implemented with five different simulation runs, one for each M^* pair.

While survival of parr is likely to be size-dependent, which could also be modeled with five values for the river $((M_{r,0}(a_r, i),\ M_{r,1}(a_r, i)))$ pair, I choose to use constant natural mortality $(M_{r,1} = 0)$ in order to focus on the affect of variable at-sea natural mortality. Thus, all five of the M^* values are only calculated for at-sea fish.

I include two additional natural mortality terms $M_{oe}(i)$ and $M_{re}(i)$ associated with the transition of parr into the ocean and spawners into the river, respectively. Therefore, inde-

pendent of fishing, survival of parr with river age a_r from river i that transition to at-sea fish is given by $e^{-M_o(a_r,0,i)-M_{oe}(i)}$, while spawners from natal river i returning to the river from the ocean have the survival rate $e^{-M_{re}(i)}$. The migrations between the river and the ocean expose fish to a wide array of habitats and thus a broader range of stressors, predators, and diseases, than at the non-migratory life history stages. I represent this increased mortality exposure through the mortality terms mentioned.

I choose a constant fishing rate $\mathcal{F}$ for this simulation to highlight the accuracy of the assessment model in this illustrative scenario. Although this rate is size selective and temporally and spatially variable in the physical world, this simplification allows me to focus on the influence of variable ocean natural mortality.

Population Dynamics

For each life history stage, the order of the life history events within a time step is migration, survival, and growth.

In my model at-sea salmon at each time step t experience natural mortality and fishing pressure, and thus total ocean mortality $Z(a_r, a_o, i) = M_o(a_r, a_o, i) + \mathcal{F}$. Fishing only occurs in the open ocean, where the stock is well mixed (i.e., fish from a particular river cannot be targeted, populations are interspersed). I let $A(a_r, a_o, t, i)$ denote the number of at-sea salmon of river age a_r, ocean age a_o, from natal river i, at time t. Since $1 - h(i)$ is the fraction of at-sea fish that do not return to the river to spawn and $g(i)$ is the proportion of parr that leave the river for the ocean, the dynamics of at-sea numbers are

$$A(a_r, a_o, t, i) = A(a_r, a_o - 1, t - 1, i) \cdot e^{-Z(a_r,a_o-1,i)} \cdot \Big(1 - h(i)\Big) \tag{6}$$

$$A(a_r, 1, t, i) = P(a_r, t - 1, i) \cdot e^{-Z(a_r,0,i)-M_{oe}(i)} \cdot g(i). \tag{7}$$

Equation (7) describes the number of new at-sea salmon of river age a_r, from natal river i, at time t.

The total number of spawners in a particular river i at time t depends on the fraction

of at-sea fish that returned the previous time step, where there is a minimum river age of 1 and a minimum ocean age of 1 before the fish are able to return and spawn. To account for straying, I let $b(i', i)$ denote the probability that an individual born in river i' returns to river i to spawn (i.e., fidelity). I assume $b(i, i) >> b(i', i)$ for $i' \neq i$ since only a small proportion of the population typically strays (Quinn, 2005). The at-sea fish that return to become spawners navigate the river to spawn before experiencing mortality and thus only encounter the natural mortality associated with returning to the river. The total number of spawners in river i at time t is

$$S_T(t, i) = \sum_{a_r=1}^{a_{r,max}} \sum_{a_o=1}^{a_{o,max}} \sum_{i'=1}^{n} b(i', i) \cdot h(i') \cdot A(a_r, a_o, t-1, i') \cdot e^{-M_{re}(i)}. \tag{8}$$

The summations over a_r and a_o account for a variety of river and ocean age combinations for fish that may be returning to spawn this year. The summation over natal rivers i' is necessary since fish can return to a non-natal river to spawn.

The total number of eggs in river i at time t from individuals born in river i' depends upon the total number of spawners $S(t, i', i)$ from natal river i' that return to river i. I compute this from Equation (8) by removing the inner summation over the rivers:

$$S(t, i', i) = \sum_{a_r=1}^{a_{r,max}} \sum_{a_o=1}^{a_{o,max}} b(i', i) \cdot h(i') \cdot A(a_r, a_o, t-1, i') \cdot e^{-M_{re}(i)}. \tag{9}$$

For the purposes of this effort, I assume fish that return to their non-natal river have decreased reproductive success (Quinn, 2005). I let $\alpha(i', i)$ denote the maximum reproductive potential of the spawner from natal river i' that returned to the current river i to spawn before density dependence acts. I set $\alpha(i, i) = 1$ for spawners returning to their natal river. I use a regional allometric equation to convert from length to weight (Equation 3) and the gonadosomatic index (GSI) δ for Chinook salmon to determine gonad mass relative to total body mass. Then using egg mass w_E, I deduce the number of eggs a spawner of a given weight can produce before density dependence acts. $E_T(t, i)$ represent the maximum number

of eggs in river i at time t:

$$E_T(t,i) = \sum_{i'=1}^{n} \frac{S(t,i',i) \cdot \alpha(i',i) \cdot \delta \cdot W(a_r, a_o, i)}{w_E}. \tag{10}$$

I consider two kinds of density dependence. In addition to the usual Ricker-style effects of spawners on parr production, I allow less than 100% fertilization. If the number of females one male can fertilize is K_{fm}, and the total number of male and female spawners returning are $S_{T,m}(t,i)$ and $S_{T,f}(t,i)$, respectively, the fraction of eggs fertilized is

$$\rho(t,i) = \min\left[1, \frac{K_{fm} \cdot S_{T,m}(t,i)}{S_{T,f}(t,i)}\right]. \tag{11}$$

Assuming Ricker recruitment, the number of new parr $P(0,t,i)$ in river i at time t is determined by the density dependence $\beta(i)$ acting on the total spawners $S_T(t,i)$, as well as the Ricker parameter $\gamma(i)$, the total number of eggs in the river $E_T(t,i)$, and the fraction of eggs fertilized $\rho(t,i)$:

$$P(0,t,i) = \rho(t,i) \cdot \gamma(i) \cdot E_T(t,i) \cdot e^{-\beta(i) \cdot S_T(t,i)}. \tag{12}$$

The number of parr in river i at time t depends on the natural mortality rate $M_r(a_r - 1, i)$, which is the only form of mortality they encounter, as well as the proportion of parr that do not migrate to the ocean, $1 - g(i)$. $P(a_r, t, i)$ is the number of parr of river age a_r from natal river i at time t, so that

$$P(a_r,t,i) = P(a_r - 1, t-1, i) \cdot e^{-M_r(a_r - 1, i)} \cdot \Big(1 - g(i)\Big). \tag{13}$$

Example Stock Assessment

I choose an assessment model to illustrate how the fish life history simulator can be used, thus it is particularly simple. I investigate the impacts of different implementations of the natural mortality rate within the simulator while holding this rate constant within the assessment.

Additionally, I vary the length of the catch time series that is input into the assessment in order to test the influence of the amount of data available.

I use Mohr (2006b), a cohort reconstruction, to motivate the assessment. The simulator and the reconstruction model are parameterized with biologically relevant values similar to those of Chinook salmon (*O. tshawytscha*) and coho salmon (*O. kisutch*). I run the simulator to steady state without fishing to avoid transient dynamics, and then introduce fishing for 20 years. Mohr (2006b) performs a reconstruction on a monthly time scale, but I choose an annual time-step for the simulator to decrease model complexity and to illustrate how the simulator and the reconstruction method interact. Many parameters in the reconstruction (Mohr, 2006b) relating to handling mortality and hatchery populations are set to zero in my assessment since these parameters, while biologically important, are not necessary for testing the assessment tool.

The simulated data used in this assessment are those of annual escapement (spawners) $S_T(a_T, t)$, similar to Equation (8), and catch $Y(a_T, t)$, both grouped by total age and measured in number of fish. For a physical stock, these data can be determined from coded-wire tags (CWTs) and sampling. Since these data are a function of total age, I introduce an indicator function $I_{a_r+a_o-a_T}$ such that

$$I_{a_r+a_o-a_T} = \begin{cases} 1 & \text{if } a_r + a_o - a_T = 0 \\ 0 & \text{otherwise.} \end{cases} \tag{14}$$

The purpose of this function is to allow only those data for fish with river and ocean ages that sum to the total age of interest to be included. For instance, if I want all the fish of total age 4, then I must include fish with river age 1 and ocean age 3, river age 2 and ocean age 2, as well as river age 3 and ocean age 1; all other age combinations would be excluded. Therefore annual escapement is

$$S_T(a_T, t) = \sum_{a_r=1}^{a_{r,max}} \sum_{a_o=1}^{a_{o,max}} \sum_{i'=1}^{n} \sum_{i=1}^{n} I_{a_r+a_o-a_T} \cdot b(i', i) \cdot h(i') \cdot A(a_r, a_o, t-1, i') \cdot e^{-M_{re}(i)}. \tag{15}$$

The annual yield is calculated by determining the number of fish that were removed from the at-sea population through both fishing and natural mortality, adjusted by the proportion of fish removed due to fishing alone, summed over natal river, for river and ocean age combinations that sum to total age:

$$Y(a_T, t) = \sum_{a_r=1}^{a_{r,max}} \sum_{a_o=1}^{a_{o,max}} \sum_{i=1}^{n} I_{a_r+a_o-a_T} \cdot \frac{\mathcal{F}}{Z(a_r, a_o, i)} \cdot \left(1 - e^{-Z(a_r,a_o,i)}\right) \cdot A(a_r, a_o, t, i). \quad (16)$$

Alternatively, in the physical world we may know some fraction of the yield from tagged/marked fish (e.g., CWTs).

Cohort Reconstruction

The purpose of the cohort reconstruction is to estimate annual ocean abundance. The model works backward through time, starting with the most recent escapement and catch data, to determine previous abundances. It only calculates ocean abundance. The reconstruction is based on total age, denoted a_T in the simulator, but I will call this a within the reconstruction, ranging from 2 to 7 years. The functions of the reconstruction are the impacts of fishing by age and year $I(a, t)$, the age-specific number of mature fish at the end of the year (escapement) $S_T(a, t)$, the estimated age-specific ocean abundance for the next year $\hat{A}(a + 1, t + 1)$, and the constant natural mortality rate $M_0(1)$ corresponding to the $M^*(1) = (M_0(1), 0)$ natural mortality case above. $M_0(1)$ is the value for the natural mortality rate in each reconstruction, unlike in the simulator where five simulation runs are performed each with a unique natural mortality rate (see Table 2 for a full list of differences between the stock assessment and the simulator). The natural mortality rate in the assessment results in the same survival to maximum age as that used in the simulator. The variable t represents the time-step in years. The impact of fishing is the total catch in my model since I have no mortality from incidental mortality from contact with equipment or predation of fish on the line. Therefore, $I(a, t)$ reduces to $Y(a, t)$. In the assessment $S_T(a, t)$ describes total spawners, and this is equivalent to escapement since it is the number of fish

that return to the river. The equation for the cohort reconstruction is

$$\hat{A}(a,t) = \begin{cases} Y(a,t) + e^{M_0(1)} \cdot (S_T(a,t) + \hat{A}(a+1,t+1)) & \text{for } a = 2,...,7 \\ 0 & \text{for } a \geq 8. \end{cases} \tag{17}$$

This equation is motivated from $\hat{A}(a+1,t+1) = e^{-M_0(1)} \cdot (\hat{A}(a,t) - Y(a,t)) - S_T(a,t)$, which is then solved for $\hat{A}(a,t)$.

One additional set of parameters I require in order to perform the reconstruction is $\hat{A}(a,T+1)$, where T is the final year of yield and spawner data (Figure 5). I will refer to these parameters as the final condition. Since the reconstruction is iterative, in order to start the reconstruction I need to calculate $\hat{A}(a,T) = Y(a,T) + e^{M_0(1)} \cdot (S_T(a,T) + \hat{A}(a+1,T+1))$, however I do not know $\hat{A}(a+1,T+1)$. I investigate a range of values for this set of parameters, including those used by Mohr (2006b), to determine the influence of these parameters (see Appendix B for details). However, for the remainder of the results reported here, in the interest of determining the "optimal" results by using the most accurate population data, I use the true simulated values for the final condition, which are determined by extending the length of the simulation.

In an ideal situation, stock assessments would be performed when a stock is first exploited. However, assessments are typically first executed much later than the start of the fishery, and often after the stock has substantially decreased in size. I perform a stock assessment both when the fishery is initialized and five years after. This allows me to investigate the importance of catch time series length in determining population estimates from the assessment, an aspect of data richness.

Bias Metric

I use a bias function, $\phi(a,t)$, to quantify the inaccuracy of the assessment model estimates. The function measures the level of error present by computing the relative difference between the estimated abundance, $\hat{A}(a,t)$, and the true simulated abundance, $A(a,t)$, with units

in number of adults. In order to easily compare between results in separate assessment scenarios, I calculate the absolute mean of the bias ($\bar{\phi}$) across age and time as a benchmark statistic:

$$\phi(a,t) = \frac{\hat{A}(a,t) - A(a,t)}{\hat{A}(a,t)} \tag{18}$$

$$\bar{\phi} = \sum_{a=2}^{a_{max}} \sum_{t=1}^{t_{max}} \frac{|\phi(a,t)|}{(a_{max} \cdot t_{max})}. \tag{19}$$

The bias function can be rewritten into the more intuitive Equation 20. This version allows me to easily relate the estimated value to the true value. For instance, a bias value of $\phi(a,t) = 0.2$ would result in $\hat{A}(a,t) = 1.25 \cdot A(a,t)$, signifying that the abundance estimate is 25% greater than the true value. I can extend this form to $\bar{\phi}$ to make statements about the percentage of overestimation or underestimation on average across age and time:

$$\hat{A}(a,t) = \frac{A(a,t)}{\big(1 - \phi(a,t)\big)}. \tag{20}$$

Results

The population dynamics are qualitatively similar for the at-sea fish across the range of natural mortality rates (see Appendix C for details). There is a decreasing linear trend in bias in ocean abundance with age when aggregated across years (Figure 6, natural mortality scenario $M^*(3)$, although the remaining scenarios are qualitatively similar). The decreasing linear trend with increasing age is caused by the structure of the reconstruction. For age 7 fish at time t, $\hat{A}(8, t+1) = 0$, and therefore $\hat{A}(7,t)$ is determined by yield, escapement, and mortality. However, if error (specifically overestimation) is present in this term, it propagates to subsequent terms. When the bias is not on average zero, as this error propagates it accumulates additional error that is all passed to the age 2 fish. The bias in ocean abundance aggregated across total age is greatest in the earliest years, while by year 5 we see the bias stabilizing and remaining roughly at 0.15 with a similar range across years (Figure 7, natural

mortality scenario $M^*(3)$). This trend can also be attributed to the backward iterative structure of the reconstruction. In the early years during which fishing is occurring the yield and resulting population dynamics are changing more rapidly, while these values have stabilized after this initial period. This results in more variable inputs to the reconstruction, in the form of yield and escapement, for the first 5 years assessment, and thus more variable bias values.

There is a clear increasing trend for the average absolute bias (Equation 19) for each of the natural mortality scenarios (Figure 8). Even when the assessment and the simulator use the same natural mortality rate, from scenario $M^*(1)$, the average absolute bias value is not negligible. There is a baseline average absolute bias value, given when $M_1(1) = 0$, due to an inherent mismatch between the simulated population and the cohort reconstruction (leftmost point in Figure 8). Although the average absolute bias increases as the natural mortality rate within the assessment becomes more dissimilar from that used in the simulator, the inherent differences between the structure of the simulated population and that of the assessment method result in an underlying average absolute bias. From the bias calculation in Equation 20, these average absolute bias values are roughly equivalent to a 24% average overestimation of the true ocean abundance.

To investigate the effects of data richness, I vary the length of the time series data input into the assessment. Since the salmon cohort reconstruction is a backward solving iterative process, providing a shorter time series simply shortens the length of the reconstruction. Patchy data are difficult to implement in the reconstruction and require further estimation before this assessment method can be used. I investigate the influence of shorter time series by removing the first 5 years of data, which simulates a fishery that was not assessed when it first opened. The bias in ocean abundance, aggregated across time, for this shorter time series is almost identical to Figure 6, however the range of each box plot is smaller. The bias aggregated across total age will be the same as that for Figure 7 with years 1-5 removed.

The average absolute bias results for the shortened time series are also shown in Figure 8. The bias values across the mortality scenarios all shift down a similar quantity, and a baseline average absolute bias value for the $M^*(1)$ natural mortality scenario is maintained (leftmost triangle in Figure 8). From Equation 20 I find that these average absolute bias values correspond to a roughly 22% average overestimation of the true ocean abundance.

Discussion

Performing a stock assessment involves making assumptions about the implemented model and the stock, based upon available data. When the assumptions within a stock assessment do not match the true dynamics of a species, or too little data are available, an increasing disparity between the abundance estimated by the assessment and the true abundance is expected. I present a tool for quantifying the robustness of stock assessment estimates by identifying these disparities, over a range of available data. Through simulation and implementation of a stock assessment I demonstrate that a significant disparity can arise for salmon stocks.

The disparity is present even when natural mortality is assumed constant in the simulator and the assessment model, which indicates further sources of error in the estimates. The simulator contains important dynamics that are not present in the assessments, including a complex age structure (following river and ocean ages) that influences growth, and thus ultimately reproduction and abundance. For instance, within the simulator two fish can have a total age of 5, but one may have had one year in the river and four years in the ocean while the other had two years in the river and three years in the ocean, resulting in different growth trajectories. Also, there are multiple life history stages, not just the adults that are considered in the assessment tool, which contribute to the overall population. For example, the salmon cohort reconstruction makes no attempt to relate spawners and recruitment, which influence the number of new parr in the population, and ultimately the number of new

at-sea fish in the population. By focussing solely on the at-sea life history stage, information is lost using the salmon assessment tool. Similar to the Namibian hake fishery mentioned in the introduction (Hilborn and Mangel, 1997), the choice of assessment model imposes restrictions on which parameters can be specified a priori, which data can be included, and thus what types of uncertainty are present in the results.

Due to the backward iterative nature of the cohort reconstruction, removing the early years of data does not substantially influence the results, however alternative catch time series may yield more influential results.

Across the two data sets and the five natural mortality rates, I observe a tendency toward overestimation, which can have more dramatic impacts on the populations in terms of overfishing, as opposed to an underestimation of the population, which would likely result in economic loss for fishermen (these conclusions are confirmed for *Sebastes* by D. Hively (Brown and Hively, 2011)). When the abundance of a stock is reported as larger than it truly is, due to overestimation within the stock assessment, this will likely lead to greater catch limits. These inflated catch limits have the potential to allow overfishing. Since the stock assessment continues to overestimate the true abundance, the consequences of overfishing may be unobserved for some time, compounding the problem and further threatening the stock. Overestimation is propagated through the salmon assessment due to the additive nature of the assessment; once one term is overestimated it can propagate for 5 time steps. This overestimation within this assessment is alarming. Care must be taken in the use of population estimates from assessment tools that tend to overestimate true abundances.

I show that careful consideration must be made when collecting and using data for analyses, since the type of data is just as important as the amount of data. Improving data poor fisheries will involve more than just expanding the length of the time series of data. The type of data needs to be appropriate for the life history considerations of that species, and must capture any consequential impacts on the population. Decreasing uncertainty will

involve obtaining improved data, which will allow for more applicable models to be used.

Although previous studies have considered the importance of different types and amounts of data for assessments (Brooks et al., 2010; Wang et al., 2009), I am not aware of any that address the issue of stock assessment robustness and data richness through the use of a life history simulator. With further work I anticipate the ability to discover species-specific thresholds of data that ensure reasonable assessment accuracy. This also has the potential to assist in data collection by specifying which types of data are most valuable for specific stocks. The simulator can also be applied to other fisheries of interest with reparameterization.

Future applications of this simulator include analyzing the effectiveness of more complex assessments and comparing assessment results for more data rich scenarios. Stock assessments with age or size composition may yield considerably different results. These results will help to identify the weaknesses of current methods in order to inform the implementation of future stock assessment methods, which will lead to improved policy decisions.

Chapter 2: A Management Problem: Predicting Effort for a Forecasted Quota for Fall-run Chinook Salmon

Introduction

The management of Chinook salmon ocean fisheries off the West coast of the United States is done in one of two ways, by specifying the number of days the fishery will be open (the primary method, known as "days open fisheries") or by specifying the quota or the allowable number of fish to be removed (known as "quota fisheries"). The management problem I investigate focuses on the latter management method. Additionally, these management strategies are region- and month-specific.

For a quota fishery within a particular management region, a quota is set for that month and fishing continues until the quota is met. Fisheries managers are interested in forecasting (predicting) the fishing effort (measured in vessel days) necessary to achieve the desired quota. When considering a single stock within a management region, the forecasted effort can be determined using historical data and current population dynamic models. However, when considering multiple well-mixed stocks (i.e,. fishermen cannot target a particular stock in the ocean), this problem because more difficult. Each stock is modeled separately using different population dynamic models. Since these models do not share information, there is no guarantee that the individual effort values calculated from each of these models will be similar. However, under the well-mixed assumption the fishing effort across the stocks should be identical. Developing a single model that incorporates all of the population dynamics for each stock into a single set of dynamics would result in a loss of information. Since the stocks have data reported at different time scales (see below for details), and appear to have separate dynamics, combining the stocks under one model would mask the individual stock dynamics and ultimately reduce accuracy.

The particular management problem I investigate is for commercially caught fall-run Chinook salmon (*Oncorhynchus tshawytscha*). In North America, Chinook salmon historically range as far south as Central California and as far north as Kotzebue Sound, Alaska (Groot and Margolis, 1991). The Pacific Fishery Management Council (PFMC) has identified seven geographical regions (management regions) off the coasts of Oregon and California that are managed on a month-specific basis (Figure 9). These management areas are: Northern Oregon (NO), Coos Bay (CO), Klamath Management Zone (KMZ) Oregon (KMZ-OR or KO), KMZ California (KMZ-CA or KC), Fort Bragg (FB), San Francisco (SF), Monterey (MO). Within these regions, three different fall-run stocks are considered to be present: Klamath River fall Chinook (KRFC), Sacramento River fall Chinook (SRFC), and "Other Chinook" (OC) that are Chinook salmon that do not originate in the Klamath or Sacramento rivers and constitute a very small proportion of the combined stocks. While the exact ocean distribution of fall-run Chinook salmon is an active research topic, KRFC and SRFC are nearly all caught south of Cape Falcon, Oregon (Mohr, 2006b; M. O'Farrell, personal communication, October 2011).

For each of these stocks, managers are confronted with different sources of uncertainty in the data used to inform management decisions (data complexity/richness). For instance, there exist age-specific rates and abundance estimates for the KRFC stock, and the abundance estimates are updated monthly based on removals by fisheries and natural mortality. For the SRFC, there are no age-specific data, and the index of abundance (which can be thought of as the "maximum number of returning fish" and is a subset of the abundance) is only updated annually (see Table 3).

The overarching management goal is to calculate a single forecasted effort value that is region- and month-specific and that describes the effort necessary to achieve a forecasted quota. These forecasted values are determined before the fishing season begins (pre-season), whereas the the post-season values are determined from data collectioned during the fishing

season, and are not the focus of this work. The single pre-season (expected) effort value, incorporated in tandem with historical data, would make it possible to forecast impacts on individual stocks and even individual age classes within the stocks. This would be particularly helpful for stocks with a minimum escapement target, since accurately accounting for harvest is critical for such stocks.

I investigate the accuracy of a single combined effort estimate, given the available data, by first performing a theoretical analysis for the existing effort calculation that is performed to estimate effort for each stock separately. I verify the accuracy of this effort calculation, and I introduce and verify the accuracy of a combined stocks effort calculation. Next, I use simulation to incorporate uncertainty into the inputs for these effort calculation, and explore the accuracy of both the individual and combined stocks effort estimates.

Theoretical Analysis

Although the management problem starts by setting a quota and then strives to determine the effort to achieve that quota, I approach this problem in reverse. I set an effort, then induce fishing on the stocks to achieve a harvest. This allows me to compare the known effort value, from simulation, to the estimated effort values, and does not change the qualitative investigation of the effort calculation. Here the known (true; simulated) effort value can be thought of as the post-season effort, in the physical problem, while the estimated effort value is equivalent to the forecasted effort and contains uncertainty.

I consider a stock with constant recruitment R_i to the adult population, where there are $i = 1 \dots n$ stocks. This assumption of constant recruitment is not necessary for the following calculation, however it simplifies the population dynamics. Since the variables of interest involve harvest and effort, this assumption will not change the qualitative results. The only life history stage being modeled is that of harvestable adults (i.e., assuming all adults are of legal size) without age structure. Thus, $A_i(t)$ is the abundance of stock i at time t. Then,

the abundance at the next time step $A_i(t+1)$ depends on recruitment and the survival of the current abundance, where M is natural mortality and fishing mortality is the product of catchability q_i and fishing effort E:

$$A_i(t+1) = R_i + A_i(t) \cdot e^{-M - q_i \cdot E}. \tag{21}$$

Let $Z_i = M + q_i \cdot E$.

To incorporate age into the population dynamics, I could consider age-specific abundance $A_i(a,t)$. Thus the total abundance of stock i at time t would be the sum of the age-specific abundances for that stock, $A_i(t) = \sum_{a=1}^{a_{max}} A_i(a,t)$. However, for the following model age-specific dynamics will not be considered.

The harvest of stock i at time t, $H_i(t)$, is the proportion of the abundance that was removed from the population due to fishing (this will also be referred to as the harvest-effort relationship):

$$H_i(t) = \frac{q_i \cdot E}{Z_i} \cdot (1 - e^{-Z_i}) \cdot A_i(t). \tag{22}$$

The notation that follows is that used by the current fisheries managers for fall-run Chinook salmon, where a period (.) represents division or "per". For instance, the harvest rate (harvest per abundance) for stock i at time t is denoted $h.r_i(t)$ and is calculated as

$$h.r_i(t) = \frac{H_i(t)}{A_i(t)} = \frac{q_i \cdot E}{Z_i} \cdot (1 - e^{-Z_i}). \tag{23}$$

And the harvest rate per unit effort (harvest per abundance per effort), $h.r.f_i(t)$, is

$$h.r.f_i(t) = \frac{h.r_i(t)}{E} = \frac{q_i}{Z_i} \cdot (1 - e^{-Z_i}). \tag{24}$$

Effort is currently estimated for each stock (estimated effort denoted f_i) by fisheries managers by taking the ratio of harvest and harvest per unit effort. This is calculated with the variables harvest, abundance, and harvest rate per unit effort as

$$f_i(t) = \frac{H_i(t)}{A_i(t) \cdot h.r.f_i(t)}. \tag{25}$$

Thus, with no uncertainty

$$f_i(t) = \frac{H_i(t)}{A_i(t) \cdot h.r.f_i(t)} = \frac{H_i(t)}{A_i(t) \cdot \frac{h.r_i(t)}{E}} = \frac{H_i(t)}{A_i(t) \cdot \frac{\frac{H_i(t)}{A_i(t)}}{E}} = \frac{H_i(t)}{\frac{H_i(t)}{E}} = E. \tag{26}$$

Therefore, the mathematical foundation for the effort calculation yields the desired effort (this calculation holds regardless of the effort-harvest relationship, see Appendix D).

I now introduce an addition effort calculation, the joint effort $f_{J:k-l}(t)$ for stocks k through l. This calculation is performed by taking the ratio of harvest and harvest per unit effort for all combined stocks of interest:

$$f_{J:k-l}(t) = \frac{\sum_{i=k}^{l} H_i(t)}{\sum_{i=k}^{l} A_i(t) \cdot h.r.f_i(t)}. \tag{27}$$

Once more, with no uncertainty

$$f_{J:k-l}(t) = \frac{\sum_{i=k}^{l} H_i(t)}{\sum_{i=k}^{l} A_i(t) \cdot \frac{h.r_i(t)}{E}} = \frac{\sum_{i=k}^{l} H_i(t)}{\sum_{i=k}^{l} A_i(t) \cdot \frac{\frac{H_i(t)}{A_i(t)}}{E}} = \frac{\sum_{i=k}^{l} H_i(t)}{\sum_{i=k}^{l} \frac{H_i(t)}{E}} = \frac{\sum_{i=k}^{l} H_i(t)}{\frac{1}{E} \cdot \sum_{i=k}^{l} H_i(t)} = E. \tag{28}$$

Thus, given perfect information in harvest, abundance, and harvest rate per unit effort, these two types of effort estimate calculations $f_i(t)$ and $f_{J:k-l}(t)$ all recover the original effort value.

Now that I have analytically determined that the underlying mathematics for these effort estimate calculations result in the desired true effort value, I will demonstrate that when using real data the individual effort estimates fail to agree across stocks.

Calculations with Data

Using the forecasted data for the months and areas where quotas were set in 2010, I calculate the individual effort estimates for both the Sacramento River Fall Chinook and the Klamath River Fall Chinook stocks, as well as the joint value for these two stocks (Figure 10; data courtesy of M. O'Farrell). Across the range of areas and months there is a wide range

between the individual effort estimates. For the California Klamath Management Zone region for instance, the SRFC and KRFC effort estimates are relatively similar across months, while in the Fort Bragg region for the months of July and August, the effort estimate for SRFC is much larger than that for the KRFC. Also, the joint estimate fluctuates, where it is more similar to the SRFC values (Monterey region), or the KRFC values (Oregon Klamath Management Zone region). This is due to the relative values of the numerators and denominators for each individual effort estimate. Also note that the KRFC estimated effort value is always less than that for the SRFC, this is due in part to the SRFC stock contribution to the quota being greater than the KRFC stock contribution for each month and area. However this alone is not enough to explain this trend. The remaining inputs for the effort calculation, abundance and harvest rate per unit effort, are not consistently larger for one stock or the other; it is the particular combinations of the effort calculation inputs that lead to consistently larger effort estimates for the SRFC stock.

From Figure 10, it is clear that there is a disparity between the estimated efforts for these stocks. The effort calculation works with perfect information and in a single stock context. However, with imperfect information (uncertainty in the data) and across multiple stocks where information is not shared between stocks, it fails to produce similar effort estimates. However, "problems are not solved by ignoring them" (Feller, pg. 12, 1971). Therein lies my motivation for this effort. I return to my theoretical work and introduce uncertainty into simulated stocks to determine how perturbations affect the individual and combined stocks effort estimates.

Simulations and Uncertainty

Within the current effort calculation used in management, the numerator is actually calculated by taking the proportion of the quota for the combined stocks that is expected for a

particular stock. If I let $H(t)$ denote the total harvest for all stocks as $H(t) = \sum_{i=1}^{n} H_i(t)$, then the proportion of the total harvest (quota) expected for stock i is

$$p_i(t) = \frac{H_i(t)}{H(t)}. \tag{29}$$

I can then recover the numerator defined in the previous section as the product of the proportion and the total harvest $p_i(t) \cdot H(t) = \frac{H_i(t)}{H(t)} \cdot H(t) = H_i(t)$. This notational difference becomes important when $p_i(t)$ is not estimated perfectly; then error is introduced into the numerator of the effort calculation, which is now calculated as

$$f_i(t) = \frac{p_i(t) \cdot H(t)}{A_i(t) \cdot h.r._i(t)}. \tag{30}$$

In the next section I explore the impact of uncertainty in this proportion, for two stocks.

2 Stock Case: Distribution

For my simulated populations for the two stock case, I have proportions $p_1(t)$ or $p_2(t) = 1 - p_1(t)$ of the entire harvest $H(t) = H_1(t) + H_2(t)$ that belong to stock 1 or 2, respectively. The time dependent component for $p_i(t)$ is important, since the individual and total harvests are changing over time. I place a distribution around $p_1(t)$ to add uncertainty into the effort calculation. Using a Beta distribution I create a random variable $\tilde{p_1}(t)$ such that $E\{\tilde{p_1}(t)\} = p_1(t)$ and $Var\{\tilde{p_1}(t)\} = \sigma^2$. The Beta distribution has parameters $\alpha(t)$ and $\beta(t)$, such that

$$E\{\tilde{p_1}(t)\} = \frac{\alpha(t)}{\alpha(t) + \beta(t)} = p_1(t) \tag{31}$$

$$Var\{\tilde{p_1}(t)\} = \frac{\alpha(t) \cdot \beta(t)}{(\alpha(t) + \beta(t))^2 \cdot (\alpha(t) + \beta(t) + 1)} = \sigma^2. \tag{32}$$

Now, with two equations and two unknowns, I can calculate $\alpha(t)$ and $\beta(t)$ in terms of $p_1(t)$ and σ^2.

From Equation 31, I can solve for β (in this derivation I drop the t dependency for simplicity) such that $\beta = \alpha \cdot (\frac{1}{p_1} - 1)$. Substituting this into Equation 32 I obtain

$$\frac{\alpha \cdot \alpha \cdot (\frac{1}{p_1} - 1)}{(\frac{\alpha}{p_1})^2 \cdot (\frac{\alpha}{p_1} + 1)} = \sigma^2, \tag{33}$$

which reduces to

$$\alpha(t) = \frac{p_1(t)}{\sigma^2} \cdot (p_1(t) \cdot (1 - p_1(t)) - \sigma^2), \tag{34}$$

since

$$\beta(t) = \alpha(t) \cdot \frac{1 - p_1(t)}{p_1(t)}. \tag{35}$$

Then the random random variable $\tilde{p_1}(t) \sim \text{Beta}(\alpha(t), \beta(t)) = \text{Beta}\ (\frac{p_1(t)}{\sigma^2} \cdot (p_1(t) \cdot (1 - p_1(t)) - \sigma^2), \frac{(1-p_1(t))}{\sigma^2} \cdot (p_1(t) \cdot (1 - p_1(t)) - \sigma^2))$ is fully defined by specifying $p_1(t)$ and σ^2.

I draw a random variable $\tilde{p_1}(t)$ to use in Equation 30 to calculate the $f_1(t)$ estimate, and $\tilde{p_2}(t) = 1 - \tilde{p_1}(t)$ for $f_2(t)$. The $\tilde{p_i}(t)$ values introduce uncertainty into both the individual and the joint stock effort calculations; $p_i(t)$ is the true proportion of stock i and can be thought of as the value calculated after the season has closed in the physical management problem, while $\tilde{p_i}(t)$ is the forecasted value that is a perturbation of the true value due to uncertainty. Although the quota is known perfectly and always achieved in the physical world, the calculation for $p_i(t)$ is based on historical proportions and has uncertainty since the proportion of the quota that is from SRFC, for instance, is not always consistent from year to year for a particular month and region. Thus, it is appropriate to perturb this value within the simulation, while keeping $H(t)$ perfectly known. Uncertainty can also be included in the abundance estimates and the harvest rates; this is discussed later.

The joint effort calculation for all the stocks in the region, however, reduces to the true effort value. Since the sum of the $\tilde{p_i}(t)$ is 1, the uncertainty in $\tilde{p_i}(t)$ is irrelevant. That is,

for an arbitrary number of total stocks

$$\begin{aligned}
f_{J:1-l}(t) &= \frac{\tilde{p_1}(t) \cdot H(t) + \tilde{p_2}(t) \cdot H(t) + \cdots + \tilde{p_l}(t) \cdot H(t)}{A_1(t) \cdot h.r.f_1(t) + A_2(t) \cdot h.r.f_2(t) + \cdots + A_l(t) \cdot h.r.f_l(t)} \\
&= \frac{\sum_{i=1}^{l} \tilde{p_i}(t) \cdot H(t)}{A_1(t) \cdot \frac{h.r_1(t)}{E} + A_2(t) \cdot \frac{h.r_2(t)}{E} + \cdots + A_l(t) \cdot \frac{h.r_l(t)}{E}} \\
&= \frac{H(t)}{A_1(t) \cdot \frac{\frac{H_1(t)}{A_1(t)}}{E} + A_2(t) \cdot \frac{\frac{H_2(t)}{A_2(t)}}{E} + \cdots + A_l(t) \cdot \frac{\frac{H_l(t)}{A_l(t)}}{E}} \\
&= \frac{H(t)}{\frac{1}{E} \cdot \sum_{i=1}^{l} H_i(t)} \\
&= \frac{H(t)}{\frac{1}{E} \cdot H(t)} \\
&= E.
\end{aligned}$$

Therefore, if all of the stocks are included in the joint effort estimate calculation, then even with uncertainty in the proportion of the total harvest that can be attributed to each stock, the true effort value is obtained.

2 Stock Case: Results

I estimate the effort for stocks 1 and 2, across time, using the perturbed proportion values $\tilde{p_1}(t)$ and $\tilde{p_2}(t)$ for standard deviation σ between 0.01 and 0.26 (this limit in σ constrains the shape of the Beta distribution to have an internal maxima). In addition to the two individual effort estimates, I also calculate the mean of the estmates $f_K(t) = \frac{\sum_{i=1}^{l} f_i(t)}{l}$ for comparison.

The range of effort estimates increases as the variance increases for stock specific effort estimates $f_1(t)$, $f_2(t)$, and $f_K(t)$

In Figure 11 I show $f_1(t)$, $f_2(t)$, and $f_K(t)$, for 3 variance values (corresponding to the standard deviation values 0.01, 0.13, and 0.26). Since $f_J(t)$ is E, these points are not plotted. We see that the range of effort values increases as the variance increases, as expected. To summarize these effort estimates, I calculate the average absolute relative error for each

variance scenario W_{i,σ^2} for $i = 1$, 2, and K:

$$W_{i,\sigma^2} = \frac{1}{T}\sum_{t=1}^{T}\frac{|f_i(t) - E|}{E}. \tag{36}$$

These values are displayed in Figure 12.

To investigate the relationship between $f_1(t)$ and $f_2(t)$, I plot these variables against each other (Figure 13). Small values of $f_1(t)$ correspond to large values of $f_2(t)$, and vice versa as a result of the relationship between $\tilde{p_1}(t)$ and $\tilde{p_2}(t)$. Also, as the effort estimates approaches the true effort (100), for either stock, the variability in estimates decreases. Beyond these observations, I do not have further intuition for what is causing the interesting "scissor" type of pattern observed in this figure.

Since my ultimate goal is to predict the true effort value from the available data, I investigate relationships between the uncertainty in the data and the resulting effort estimate. I find that the ratio of the perturbed and true proportions ($\frac{\tilde{p_i}(t)}{p_i(t)}$) plotted against the estimated and true effort values ($\frac{f_i(t)}{E}$) for each stock, result in a line with a slope of 1 and an intercept of 0 (the "$y = x$" line). This demonstrates that the uncertainty in the proportion of the total harvest that can be attributed to each stock is propagated, unchanged, throughout the effort calculation. These results may be more illuminating in the three stock case, if the joint effort calculation for two stocks can be related to the error in the calculated value.

For all but the smallest absolute relative error values, the mean does out perform the individual estimate (Figure 14). The same pattern is observed when the individual estimates are for stock 2. I plot the absolute relative error (the W_{i,σ^2} values before they are averaged over time) against the mean absolute relative error, where the error is normalized to fall between 0 and 1. If the mean estimates were an improvement on the individual estimates, we would expect to see all of the points falling below the $y = x$ line, since this indicates that the mean estimate produced a smaller absolute relative error than that produced by the individual estimate.

3 Stock Case: Distribution

Now I consider a scenario with three stocks. Since the generalization of the Beta distribution is the Dirichlet distribution, I can add uncertainty to the proportions $p_1(t)$, $p_2(t)$, and $p_3(t)$ using a Dirichlet: $(\tilde{p_1}(t),\ \tilde{p_2}(t),\ \tilde{p_3}(t)) \sim \text{Dirichlet}(\alpha_1(t), \alpha_2(t)), \alpha_3(t))$. The restrictions on the Dirichlet distribution are as follows: $0 \leq p_i(t) \leq 1$ for all i; $\sum_{i=1}^{3} p_i(t) = 1$; and $\alpha_i(t) > 0$ for all i.

To calculate the $\alpha_i(t)$ parameters for this distribution, I first define the expectation for each random variable to be the true proportion value such that $E\{\tilde{p_i}(t)\} = p_i(t)$. Setting $\alpha_0(t) = \alpha_1(t) + \alpha_2(t) + \alpha_3(t)$, I can write each expectation by definition as

$$E\{\tilde{p_i}(t)\} = \frac{\alpha_i(t)}{\alpha_0(t)} = p_i(t). \tag{37}$$

However, since $p_3(t) = 1 - p_1(t) - p_2(t)$, the equation for $E\{\tilde{p_3}(t)\}$ does not add any additional information and can be derived from the equations for $E\{\tilde{p_1}(t)\}$ and $E\{\tilde{p_2}(t)\}$. Therefore, I have two equations and three unknowns and I must define another equation to solve this system. I define the variance for $\tilde{p_1}(t)$ as $Var\{\tilde{p_1}(t)\} = \sigma^2$ for my third equation, so

$$Var\{\tilde{p_1}(t)\} = \frac{\alpha_1(t) \cdot (\alpha_0(t) - \alpha_1(t))}{\alpha_0(t)^2 \cdot (\alpha_0(t) + 1)} = \sigma^2. \tag{38}$$

Combining the equations from Equation 37, I obtain expressions for each α (dropping the time dependence for simplicity) in terms of the other α's: $\alpha_1 = \frac{p_1}{1-p_1-p_2} \cdot \alpha_3$; $\alpha_1 = \frac{p_1}{p_2} \cdot \alpha_2$; $\alpha_2 = \frac{p_2}{1-p_1-p_2} \cdot \alpha_3$. By substituting these values into Equation 38, I can obtain an equation for each unknown parameter in terms of the known values p_1, p_2 and σ^2:

$$\alpha_1(t) = \frac{p_1(t)}{\sigma^2} \cdot (p_1(t) \cdot (1 - p_1(t)) - \sigma^2) \tag{39}$$

$$\alpha_2(t) = \frac{p_2(t)}{\sigma^2} \cdot (p_1(t) \cdot (1 - p_1(t)) - \sigma^2) \tag{40}$$

$$\alpha_3(t) = \frac{1 - p_1(t) - p_2(t)}{\sigma^2} \cdot (p_1(t) \cdot (1 - p_1(t)) - \sigma^2). \tag{41}$$

Note that each $\alpha_i(t) > 0$ if $p_1(t) \cdot (1 - p_1(t)) > \sigma^2$.

Using Equations 39, 40, and 41 I can fully define the Dirichlet distribution for my random variables: $(\tilde{p_1}(t), \tilde{p_2}(t), \tilde{p_3}(t)) \sim \text{Dirichlet}(\frac{p_1(t)}{\sigma^2} \cdot (p_1(t) \cdot (1-p_1(t)) - \sigma^2), \frac{p_2(t)}{\sigma^2} \cdot (p_1(t) \cdot (1-p_1(t)) - \sigma^2), \frac{1-p_1(t)-p_2(t)}{\sigma^2} \cdot (p_1(t) \cdot (1-p_1(t)) - \sigma^2)$. At each time step, I draw the random proportions $\tilde{p_1}(t)$, $\tilde{p_2}(t)$, and $\tilde{p_3}(t)$ and use them to calculate the individual and joint effort estimates. Although the joint effort calculation $f_{J:1-3}(t)$ for all three stocks will also reduce to the true effort, as demonstrated above, I can perform the joint effort calculations on two stocks at a time resulting in the estimates $f_{J:1,2}(t)$, $f_{J:1,3}(t)$, and $f_{J:2,3}(t)$. These joint effort estimates on two stocks retain uncertainty since I am not summing all the proportions and thus removing them from the calculations as is done for the joint estimate for all yhree stocks. The joint two stock calculations are simulating the effort estimates for two observed stocks (with some observation error), when an unknown third stock is also present. Additionally, I can compare the accuracy of these effort estimates with the one stock effort estimates $f_1(t)$, $f_2(t)$, and $f_2(t)$, and the mean estimates of the stocks $f_{K:1,2}(t)$, $f_{K:1,3}(t)$, $f_{K:2,3}(t)$, and $f_{K:1,2,3}(t)$, to determine if combining stock information improves accuracy.

3 Stock Case: Results

Using the perturbed proportion values $\tilde{p_1}(t)$, $\tilde{p_2}(t)$ and $\tilde{p_3}(t)$ I estimate the effort for stocks 1, 2, and 3, respectively, for the standard deviation of $\tilde{p_1}(t)$, σ, between 0.01 and 0.32 (this limit in σ constrains $\alpha_i(t) > 0$ for all i, as required for the Dirichlet distribution). Additionally, I calculate the joint effort estimate values mentioned above, as well as multiple stock means, for a total of 10 effort estimates.

We do not see substantial differences in variability within each effort estimate across the variance values (Figure 15). The mean and joint estimates cluster closer to the true value than each of the individual effort estimates used to calculate these combined effort values. This observation holds true for the remaining variance cases not shown.

From Equation 36, I calculate the average absolute relative error for each variance value and each effort estimate type (Figure 16). The mean and joint effort estimates for two stocks

have a smaller average absolute relative error than the individual effort estimates for those same two stocks. For instance, $W_{K:1,2,\sigma^2}$ and $W_{J:1,2,\sigma^2}$ are both less than W_{1,σ^2} and W_{2,σ^2}, and the smaller the W value the closer the effort estimates are to the truth (a value of 0 corresponds to perfect agreement between the estimates and the true effort value).

I again plot the effort estimates of each stock against each other stock (Figure 17 shows these results for stocks 1 and 2, however the remaining relationships are qualitatively similar). As either stock approaches an extreme large effort estimate, the other stock approaches an extreme small effort value. This is a result of the relationship between the $\tilde{p}_i(t)$; since $\tilde{p_1}(t) + \tilde{p_2}(t) + \tilde{p_3}(t) = 1$, as one $\tilde{p}_i(t)$ gets large, the remaining $\tilde{p_j}(t)$'s must necessarily be small.

I also investigate the relationship between the joint estimates and individual stock estimates. When I consider $f_i(t)$ and $f_{J:k,l}(t)$, $k, l \neq i$, where the individual estimate was not one of those used to calculate the joint estimate (Figure 18 illustrates these results for the stock 1 effort estimate versus the joint stock 2 and 3 estimate, although the other two cases are qualitatively similar), we see an interesting pattern. As either the joint or the individual effort estimate approaches the true effort value, we see a reduction in variance. For the other cases where the individual estimate was also used to calculate the joint estimate, this does not occur.

The ratio of the perturbed and true proportions plotted against the estimated and true effort values for that stock result in a line with a slope of 1 and an intercept of 0. However, when plotting the proportion ratio against the effort ratio for the joint estimates, this does not hold true. These figures are similar to those for the individual effort estimates versus the joint estimates. The ratio of the proportion for stock i plotted against the ratio of the joint estimates for stocks k and l and the true effort produce figures that are qualitatively similar to Figure 18.

When I plot the normalized (values between 0 and 1) absolute relative error for the

individual stock and corresponding joint stock estimates, it is clear that the joint value is generally an improvement over the individual value, although not to the extent demonstrated in Figure 14 (Figure 19 depicts this relationship for stock 1 and the corresponding joint estimates for stocks 1 and 2, and 1 and 3, and the remaining figures not displayed are qualitatively similar). In Figure 20 I display the same values, however the vertical axis depicts the absolute relative error for the mean (figures not displayed are qualitatively similar). Again, I do not have intuition for what is causing the patterns we observe in these figures, other than the restriction of the $\tilde{p}_i(t)$'s to sum to one.

By imposing a probability distribution over the variance values (i.e., how likely an observed variance in $\tilde{p_1}(t)$ is), I can calculate weighted means for the average absolute relative error for each effort estimate. In Figure 21 I display three possible probability distributions for the variance values: uniform, exponentially decreasing, and normal. I then weight each average absolute relative error by the corresponding probability for that variance level, and sum these values, creating a weighted average across the effort estimate types (Figure 22).

Discussion

Through my theoretical analysis, I establish that the foundation mathematical structure for the effort estimate calculations is intellectually solid. Upon first inspection, this was not entirely clear. I initially investigated the influence of non-linear truncation of the harvest rate per unit effort. By Taylor expanding the e^{-Z_i} in the $h.r.f_i(t)$, for $Z_i << 1$, and retaining only the first two terms of the Taylor expansion, I found $h.r.f_i(t) \approx q$. However, from Equation 26 we see that the form of $h.r.f_i(t)$ is not important since the calculation reduces to the true effort.

In the two stock case, the mean of the effort estimates appears to be a viable alternative to either individual effort estimate since the mean outperforms the individual estimates in terms of minimizing the absolute relative error. In the three stock case, the joint and mean

estimates are an improvement over the individual estimates that make up the combined estimates, since the joint and mean estimates lead to smaller absolute relative errors. In fact, on average the joint estimate appears to perform better then the mean estimate.

While the three stock case most closely mirrors the scenario experienced by current fishery managers, the problem is more complex than that modeled here. For instance, there are both commercial and recreational fisheries harvesting these stocks. Additionally, the "Other Chinook" stock is comprised of many additional stocks, and data for these stocks contain additional uncertainty. While the results presented here can inform the management process in determining which effort estimate to report, the influence of uncertainty in both the harvest rates and abundance values should be further investigated. Although the majority of the uncertainty is expected to be in the proportion of total harvest attributed to each stock, the abundance estimates are also uncertain. The abundance values are used in calculating the harvest rate, and thus also contain uncertainty. By further investigating the propagation of uncertainty in additional parts of this calculation and considering additional complexity in the model, we can improve our investigation of the relationships between the estimated effort values. These results can influence future sampling efforts; if error in a particular component of the effort calculation is found to more negatively impact the effort estimates, then reducing the uncertainty in that variable through data collection would improve the estimates.

Chapter 3: A State-dependent Life History Model to Investigate Resource Allocation in Green Sea Turtles

Introduction

Life history theory proposes the existence of trade-offs between reproduction and growth, which lead to variation in life histories, including diversity across age and size at maturity, fecundity, and survival rates (Roff, 1992; Stearns, 1992). Numerous laboratory and field experiments and observational studies across many species center around investigating these trade-offs by analyzing the relationship between life history traits such as fecundity and parental survival, offspring initial size and parental or offspring survival, as well as the role of mating timing (Stearns, 1992; Forbes and Calow, 1996).

With this as motivation, I investigate the interaction between growth and detoxification for juvenile green sea turtles. The premise behind this work is that developing juvenile sea turtles that are accumulating toxins through the environment are confronted with a resource allocation "choice" (defined in the evolutionary optimal sense). Utilizing more resources for growth diminishes the resources that are available to detoxify (or repair damage), and vice versa. When this problem is considered from the standpoint of fitness, measured by the number of healthy offspring (eggs) a juvenile is ultimately expected to produce, I propose to develop a state-dependent life history model (Clark and Mangel, 2000; Mangel and Clark, 1988) to determine the optimal allocation of resources given the health (weight and damage level) of the individual.

I choose green sea turtles (*Chelonia mydas*), known regionally in Baja California Sur (BCS), Mexico as black sea turtles, for my model system for a variety of reasons. Sea turtles migrate throughout much of their life cycle and between life history stages (species dependent, up to tens of thousands of kilometers over a lifetime). They experience a variety of

habitats, and consequentially are susceptible to a greater variety of stressors. Additionally, due to their longevity (some species living over 100 years) pollutants, including organochlorines and heavy metals, tend to bioaccumulate and reach especially high concentrations (Aguirre et al., 2006). Sublethal impacts from toxins can impair feeding, immunity, growth, and reproduction (Lutz and Musick, 1997; Lutz et al., 2003; Bergeron et al., 1994).

Sea turtles experience a host of stressors and toxin exposures throughout their life cycle, which can impact growth, reproduction, and ultimately population dynamics and persistence (Lutz and Musick, 1997; Koch et al., 2006; Aguirre et al., 2006). By investigating the impact of toxins on life history traits, such as growth, I can improve our understanding of this species, seek to mitigate crucial exposer periods, and direct the focus of future data collection to help answer these questions. This work was done in collaboration with V. Labrada-Martagón, who also provided the data.

Although relationships between fitness or health and stress or toxins are loosely hypothesized, higher toxin and stress loads generally expected to negatively impact fecundity and survival. The strength of these relationships vary between individuals as well as within individuals across life history stages (Bonier et al., 2009). Since the hormones that are used to measure stress level, such as glucocorticoids or stress hormones, rarely give clear relationships to fitness due to the abundance of variation in measurements and the difficulties of repeat sampling, such measures of stress are often inconclusive. Additionally, the act of sampling from an individual typically induces stress responses and confounds results, making it nearly impossible to establish baseline levels. Differentiating chronic and acute stress can be quite challenging, especially when foundation levels are unknown (Breuner et al., 2008). Maximum toxin loads, the amount of toxin that directly causes immediate death, in addition to the current range of the level of toxin within a species are often unknown. Data collection for threatened and endangered species, such as black sea turtles, is especially difficult since it is quite challenging to procure permissions to sacrifice individuals for scientific study. Due

to the limitations and inconclusive nature of available stress and toxin data, especially for sea turtles, modeling is a natural first approach to investigating the influence of toxins.

Juvenile black sea turtles use lagoons along the coast of BCS to grow and reach maturity before migrating (Figure 23). Although foundational toxin data are limited, Labrada-Martagón et al. (2010a,b,2011) were able to collect data from 2005-2007 at three sites along BCS: Punta Abreojos (PAO), Bahía Magdalena (BMA), and Laguna San Ignacio (data not used due to small sample size) (Figure 24). These data include weight and straight carapace length, the status of the turtle (injured versus healthy), 18 biochemical parameters from blood samples, as well as heavy metal (trace elements) and organochlorine pesticides (OC) concentrations in the blood. Organochlorines, including polychlorinate biphenyls (PCBs), are associated with immune suppression and are thought to act as endocrine disrupters. The biochemical parameters examined include protein concentrations, levels of electrolytes, glucose, calcium, and enzyme activity. The trace elements measured in the sampled turtles include iron, zinc, silicon, cadmium, selenium, and magnesium. The 25 different pesticides found in these samples were categorized into seven groups including dichlorodiphenyltrichloroethanes (DDTs) and hexachlorocyclohexanes (HCHs).

The turtles sampled by Labrada-Martagón et al. (2010a,b) showed evidence of toxin contamination and body condition (health) that varied between sites, allowing for a range of data that is site specific. However, baseline values for maximum toxin load survival are to date unknown, as are the affects of particular combinations and levels of toxins. Using the Baja region data for reference values and qualitative inferences regarding habitat toxicity for the two regions PAO and BMA, I use a dynamic state variable model to investigate different allocation strategies between sites to growth and detoxification for juvenile black sea turtles.

Model

States: Weight and Damage

The states for this model are damage level $D(t)$, weight $W(t)$, and time t, where damage can be thought of as the result of short- and long-term stress from things as diverse as disease, parasites, fishing, pesticide and heavy metal exposure, and temperature changes.

From the von Bertalanffy growth equation (von Bertalanffy, 1957), I assume that resource accumulation R is a function of food quality and abundance q, metabolic costs k, and weight $W(t)$:

$$R(W(t)) = q \cdot W(t)^{\frac{2}{3}} - k \cdot W(t). \tag{42}$$

Then, if a fraction of resources α $(0 \leq \alpha \leq 1)$ are allocated to growth at time t, weight at time $t+1$ is

$$W(t+1) = W(t) + \alpha \cdot R(W(t)). \tag{43}$$

Since the model is tracking allocation to weight, but length determines maturity (discussed below), I must define an allometric length to weight relationship. Starting from the assumption that weight varies with length in the following way:

$$W(t) = a \cdot L(t)^b, \tag{44}$$

in logarithmic form this becomes $log(W(t)) = log(a) + b \cdot log(L(t))$. Using the results from Labrada-Martagón et al. (2010b), I determine the year-specific values for $log(a)$ and b for all three years of data for PAO and for two years of data for BMA. I average both the $log(a)$ and b values separately for each region to get a region-specific mean across the available years of data (see Table 4 for specific values).

From Equation 44, I can determine the length at time $t+1$:

$$L(t+1) = \frac{W(t+1)^{\frac{1}{b}}}{a}. \tag{45}$$

Note that $L(t+1) \geq L(t)$ if $W(t+1) \geq W(t)$. Thus both length and weight cannot decrease unless $R(W(t)) < 0$.

Although physically length and weight can vary independent, to limit the number of states in the fitness function and thus the degree and complexity of the model, this examination does not investigate that aspect.

The update for the damage level in the next time period depends on the conversion factor for changing resources into the components necessary to detoxify ρ, the constant accumulation of damage from the habitat c, including exposure through ingestion of contaminated resources and that in the water column, and the damage associated with fishing c_F, where fishing is represented by F. Thus the dynamics of damage are

$$D(t+1) = D(t) \cdot e^{-\rho \cdot (1-\alpha) \cdot R(W(t))} + c + c_F \cdot F. \tag{46}$$

In light of Equations 43 and 46, and given that $D(t) = d$ and $W(t) = w$, and allocation α is set, the updated values of the states at time $t+1$ are

$$w'(\alpha) = w + \alpha \cdot R(w) \tag{47}$$

$$d'(\alpha) = d \cdot e^{-\rho \cdot (1-\alpha) \cdot R(W(t))} + c + c_F \cdot F. \tag{48}$$

Dynamics: Mortality and Fitness

In order to determine the optimal allocation α^* to weight at each time step, I define

$$\begin{aligned} F(d, w, t) \;=\; & \max_{\alpha} \; E\{\text{reproductive fitness from time t to final time T} \\ & \text{for juveniles, given that } D(t) = d, W(t) = w\}. \end{aligned} \tag{49}$$

This equation is solved by iterating backward from the final time step, one time step at a time. At each iteration I calculate the reproductive fitness (defined below) associated with the given states d and w; I perform this calculation for each α value to determine the allocation that leads to maximum fitness. The result is the optimal allocation strategy for

each state and each time step (this procedure is the backward iteration; Clark and Mangel, 2000; Mangel and Clark, 1988). Once the optimal allocation is determined, dependent on the states of the turtle, a population is initialized at time $t = 1$ across a range of initial damage and weight values. The states for each turtle in the population are updated through time, where the individual allocates resources using the optimal allocation strategy at each time step (forward iteration).

I define reproductive fitness as the total number of eggs a turtle of weight w lays in her first year of reproduction $B(w)$ if that turtle has reached reproductive size l_{max} by the final time step, where length is measured as straight carapace length to be consistent with the data from Labrada-Martagón et al. (2010b). The l_{max} used in this work was that of the mean nesting size of black sea turtles since this is considered an appropriate estimate for size at maturity in females (Koch et al., 2007). Length is used to determine maturity since turtles can have very variable weights for a given length and I considered this metric more indicative of age than weight since length is rarely decreased, while weight can vary drastically dependent on health and habitat conditions.

Also, as damage level increases the total egg number should be decremented since toxins can be passed from reproductive females to their offspring, reducing the overall fitness of the offspring (Lutz et al., 2003). By defining μ_d as the rate of reduction in fitness associated with one unit of damage, the final fitness is

$$F(d, w, T) = \begin{cases} B(w) \cdot e^{-\mu_d \cdot d} & \text{if } l \geq l_{max} \\ 0 & \text{if } l < l_{max}. \end{cases} \tag{50}$$

I model the mortality rate for juvenile sea turtles with four components: a fixed baseline (size-independent) natural mortality μ_0, natural mortality inversely proportion to length (size-dependent) μ_1, fishing mortality directly proportional to length (size-dependent) μ_F, and mortality associated with the damage level μ_{d_m}. The μ_0 is included to capture death due

to disease and parasites, however conditions such as fibromyalgia are rare in the modeled regions and therefore the value used for this parameter is small. While hatchlings and young juveniles (or early juveniles;"lost years" life history stage) are thought to have the lowest survivorship, the later juvenile stage I am modeling is thought to have relatively low predation since the number and diversity of potential predators decreases with increasing size (Lutz and Musick, 1997). Additionally, the location of the habitat later juveniles inhabit also acts to prohibit large predators. Thus, μ_1 is also relatively small. However, larger length sea turtles are assumed to be targeted by illegal fishermen for the greater meat. Thus μ_F, which is the fishing mortality rate per unit fishing and per unit length, while F is the fishing rate, scales with length. As the damage level increases, it is thought to impair the ability of the sea turtle to escape fishing, as well as act as an immunosuppressant, thus exposing the turtle to a higher risk of mortality. Thus, total mortality rate is

$$\mu(l,d) = \mu_0 + \frac{\mu_1}{l} + \mu_F \cdot F \cdot l + \mu_{d_m} \cdot d. \tag{51}$$

Then, in light of Equation 49:

$$F(d,w,t) = \max_{\alpha} \begin{cases} e^{-\mu(l(w'(\alpha)),d'(\alpha))} \cdot F(d'(\alpha), w'(\alpha), t+1) & \text{if } l(w'(\alpha)) < l_{max} \\ B(w'(\alpha)) \cdot e^{-\mu_d \cdot d'(\alpha)} & \text{if } l(w'(\alpha)) \geq l_{max}. \end{cases} \tag{52}$$

This defines all of the equations that are necessary for solving the backward portion of the dynamic state variable model, which results in the optimal allocation to weight for each set of states, α^*, for each region, BMA and PAO. To perform the forward portion of the model, I must also specify the starting conditions for the individuals. For each of the two model runs (one for each region) I simulate 500 individuals all starting with damage at the minimum level and across 10 different weights (the first 10 weights for each region in Table 4; 50 individuals per weight), which are all less than the mature weight.

Results

In Figure 25 I show the optimal resource allocation α^* for each damage and weight combination for four different time steps from the PAO region. Although the weight values differ between PAO and BMA, and thus the weight binning differs between regions, the resulting figure for BMA is nearly identical. For the time steps that are not pictured, between 1 and 41, I observe stationarity where the current allocation decision is relatively insensitive to the value of t and the color maps are similar to that for time 1 (Clark and Mangel, 2000; Mangel and Clark, 1988). For time steps beyond and including time 41, the blue region on the left continues to expand to the right until the image is that depicted for time 49.

The total number of juveniles that reach maturity for the PAO and BMA models, respectively, were 25 and 46, out of 500 (the remaining individuals died from mortality; see Figures 26 and 27). For PAO, 12 individuals reach maturity at time 5, from a starting weight of 48.21 kg; 7 reach maturity at time 7, from a starting weight of 38.71 kg; 3 at time 9, from a starting weight of 30.55 kg; 1 at time 12, from a starting weight of 23.61 kg; and 2 at time 14, from a starting weight of 17.81 kg. For BMA, 21 individuals reach maturity at time 4, from a starting weight of 45.68 kg; 14 at time 6, from a starting weight of 37.20 kg; 5 at time 8, from a starting weight of 29.80 kg; 4 at time 10, from a starting weight of 23.42 kg; and 2 at time 14, from a starting weight of 13.43 kg. Individuals initialized at larger weight classes mature earlier, since they start closer to the mature weight (corresponding to the mature length). Additionally, we see no mature individuals that start with weights less than 17.81 kg for the PAO region, and less than 13.43 kg for the BMA region. This is due to the length of the time the model is run. The smallest individuals all die before they can reach maturity since it takes these individuals longer to reach maturity and there is a greater chance of mortality acting before they can reach the mature size. For instance, if survival in each time step is 80% and individual A needs 2 time steps to reach mature size while

individual B needs 6 time steps to reach the same mature size, the probability individual A survives to maturity is 0.64 while this number reduces to 0.26 for individual B. In PAO the maximum damage level is 5.4, while in BMA this value is 6.0. Therefore, only the lower third of the resource allocation matrix α^* is utilized.

I also compare the survival probabilities to reach maturity resulting from the model with those estimated for physical populations. Bjorndal et al. (2003) reported an annual survival rate of 0.761 for juvenile green turtles exposed to both human-induced and natural mortality, in the Bahamas. Using the number of years the turtles in my model took to mature (between 4 and 14; not considering regional differences), I calculate the expected survival rate to maturity for the juveniles assuming this same annual survival rate. Next I calculate how many individuals within an initial weight class reach maturity. The results of these calculations are shown in Table 5. We can see that there is relatively good agreement between these values. For instance, in the model 7 individuals matured at time 7, out of a total of 50 possible for this initial weight class. Thus, 7/50, or a proportion of 0.14 survive to maturity. The survival probability across 7 years, using the estimate from Bjorndal et al. (2003), is 0.148. Thus, the survival to maturity created from my model is similar to the value estimated from physical populations. Also, since survival is stochastic within the model, additional differences between the survival rate calculated from observed data and those determined from the model are expected.

Discussion

This work creates a framework for further modeling in which data from Labrada-Martagón et al. (2010a,b,2011) as well as other more general sources for green turtle biology can be used to inform the model. Incorporating a measure of body condition, where turtles of the same length can vary in weight based on their toxin load, would greatly increase the applicability of the results. Additionally, by breaking the toxins into two categories, heavy metals and

organochlorines, the differences in how these compounds influence sea turtle biology can be teased apart. For instance, while baseline values for some heavy metals are necessary in processes such as the production of the shells of eggs, and thus beneficial, organochlorines are not known to be beneficial at any level. By incorporating dose-response curves for each type of toxin and for the interaction of these toxins into the model, further complexity can be modeled. Additionally, the model can be calibrated against data by calculating the condition for turtles of a given length, weight, and toxin load, and comparing these to trends observed by Labrada-Martagón et al. (2010a,b,2011) for healthy and injured turtles, using the injured turtles as a proxy for turtles with heavy toxin loads since higher toxins should influence the immune response and vulnerability of these turtles. Since younger (smaller) turtles are observed to feed further in the lagoons, with a more omnivorous diet, we can also vary toxin intake by size since omnivores are eating higher in the food chain and thus ingesting more toxins than the larger herbivore juveniles. Finally, it has been shown that numerous behaviors and life history parameters, such as growth, vary by season, and thus this complexity can be included as well.

Although there is always further work that can be done to improve any model, no model will perfectly capture the dynamics in nature. This model provides a starting point for future models, while still capturing some of the dynamics we expect to see. For instance, turtles of a small size across a large range of damage values, will allocate more resources to growth. Additionally, the closer to the end time the turtles get, the more resources they allocate to growth in order to attempt to meet the minimum weight for maturity. Also, for the highest damage levels across time and weight, a large proportion of resources are allocated to removing damage. I also find that the survival rates to maturity observed in the model are similar to those obtained from physical data, demonstrating that this model can reproduce life history values from known green sea turtle biology. Extending the theory modeled here with data can inform us about the accuracy of the relationships we assume between toxins

and life history traits, as well as determine which data still needs to be collected to improve these models and thus their results and inferences. Furthermore, conclusions drawn here on the individual level can be extended and applied in population models to determine how life history traits play into population dynamics.

Understanding the sensitivity of the model to the given parameters is also important for future work and inferences. Increasing or decreasing variables such as the rate at which an individual accumulates damage and resources will influence how quickly damage can be removed, as well as influence growth. As a further study, I set the damage in the mortality rate to zero, $\mu_{d_m} = 0$, and find that this drastically changes the allocation strategy, as well as the survival of the initialized population (almost 60% of the population survived to reach maturity, including the individuals with the smallest initial sizes). The allocation strategy is almost entirely to increasing weight, across damage and weight values. Only individuals that were close to reaching mature size allocate to removing damage. Setting this parameter to zero implies that damage has no influence on the individual, except in terms of egg production (i.e., there are no sublethal effects). Thus, as the relationships between toxins, organochlorines, and life history parameters are further developed various scenarios can be implemented in this modeling technique to test the impact on allocation strategies.

Conclusions

"The purpose of models is not to fit the data but to sharpen the questions"

–Samuel Karlin from the eleventh R A Fisher Memorial Lecture at the Royal Society of London, 20 April 1983

Each of these models furthers the understanding of the problem I investigate. For the salmon life history simulator, I find that assumptions within the assessment method are influential. For the salmon assessment method I consider, the cohort reconstruction, these assumptions can lead to consistent overestimation of the abundance. Consequently, policy decisions based on these assessment results need to account for this potential inaccuracy. Results of the forecasted fishing effort modeling problem indicate that combining information, in the form of calculating a mean or joint effort estimate, leads to more accurate estimates than individual estimates. From the state-dependent sea turtle life history model, I discover a potential weight allocation strategy.

The models I present represent initial approaches to complex problems, all three have great potential for incorporating further complexity. Within the salmon simulator I could incorporate life history parameters that vary by sex as well as climate. Additionally, further developing the cohort reconstruction to include length at age data could improve the abundance estimates produced from this assessment method. For the quota-effort problem, by incorporating uncertainty in both abundance and harvest rates the model would more closely approximate the current management problem and these results could provide further insight into determining the most accurate effort estimate. Incorporating data into the juvenile sea turtle model, by explicitly modeling both the organochlorine and heavy metal loads for individuals, would provide results that are easier and perhaps more appropriate to compare with the observed system.

Beyond informing and expanding the current models using data, these models can also act as stepping stones to models that including other biological mechanisms such as selection. For the sea turtle model, for instance, a model building off of that presented here could incorporate the idea that individuals with the lowest metabolic rates respond best to environmental stress (Forbes and Calow, 1996) and that this tolerance is passed to offspring. Future generations with this low metabolic rate would be more fit for the current environment. Alternative, if the environment is altered to become less toxic, after this selection takes place, turtles that did not have low metabolic rates would out perform those with low metabolic rates. Since a decreased metabolic rate necessarily results in an increased time to reach maturity (slower growth), the reproductive dynamics of the population would likely change. By including these ideas into a larger model, we could test the impact of a changing environment on juvenile sea turtles, both individually and as a population.

These models, in their current state, expand the knowledge about the specific problem I investigate, however to obtain a deeper understanding they should be used as building blocks for further complex models. The results of these and future models can also assist in directing further data collection for targeting the most sensitive parameters within the models and the systems.

Appendix A: Life History Simulator Natural Mortality Parameters

To calculate parameter values for the salmon specific natural mortality parameters $M_{r,0}$, $M_{r,1}$, $M_{o,0}$, and $M_{o,1}$ (Equations 4 and 5; the i is removed for clarity) I first specify survival to river age a_r and ocean age a_o as $S(a_r, a_o)$. I decompose survival into two parts, survival to river age $S_r(a_r)$ and survival to ocean age conditioned on survival to the given river age $S_o^c(a_r, a_o)$:

$$S(a_r, a_o) = S_r(a_r) \cdot S_o^c(a_r, a_o). \tag{A1}$$

Since survival, excluding fishing mortality, in a single year is e^{-M_r} or e^{-M_o} depending on location, iterating this over the river and ocean ages of the fish results in two survival equations:

$$S_r(a_r) = e^{-M_{r,0}\cdot(a_r+1)-M_{r,1}\cdot\sum_{a_r=0}^{a_r}\frac{1}{Lr(a_r)}} \tag{A2}$$

$$S_o^c(a_r, a_o) = e^{-M_{o,0}\cdot a_o-M_{o,1}\cdot\sum_{a_o=1}^{a_o}\frac{1}{Lo(a_r,a_o,r)}}. \tag{A3}$$

The slight differences in these equations arise from having a minimum river age of 0 due to recruitment, whereas ocean age has a minimum of 1. Next, I choose a value for $S_o^c(a_{r,max}, a_{o,max})$ that describes the conditional survival to maximum river age $a_{r,max}$ and ocean age $a_{o,max}$. Then Equation A3 becomes

$$S_o^c(a_{r,max}, a_{o,max}) = e^{-M_{o,0}\cdot a_{o,max}-M_{o,1}\cdot\sum_{a_o=1}^{a_{o,max}}\frac{1}{Lo(a_{r,max},a_{o.max},r)}}. \tag{A4}$$

I now have one equation with two unknowns, $M_{o,0}$ and $M_{o,1}$. To make this problem tractable, I specify a range of values for $M_{o,0}$. The lower bound of this value is 0, corresponding to no size-independent mortality. To calculate the upper bound, I consider the scenario with no size-dependent mortality, $M_{o,1} = 0$:

$$S_o^c(a_{r,max}, a_{o,max}) = e^{-M_{o,0}\cdot a_{o,max}}. \tag{A5}$$

Since $S_o^c(a_{r,max}, a_{o,max})$ and $a_{o,max}$ are specified, the upper bound on $M_{o,0}$ is $M_{o,0}^u = \frac{|ln(S_o^c(a_{r,max},a_{o,max}))|}{a_{o,max}}$. Now I have the range of $M_{o,0}$: $[0, M_{o,0}^u]$. Choosing values within this range allows me to calculate the corresponding $M_{o,1}$ values. Let $M_{o,0}^*$ be a value within the range of $M_{o,0}$, then from Equation A4 the corresponding $M_{o,1}$ is

$$M_{o,1}^* = \frac{|ln(S_o^c(a_{r,max}, a_{o,max}))| - M_{o,0}^* \cdot a_{o,max}}{\sum_{a_o=1}^{a_{o,max}} \frac{1}{L_o(a_{r,max},a_{o.max},r)}}. \tag{A6}$$

The values of $M_{o,0}$ I choose for the simulator are: $M_{o,0}^u$, $\frac{3}{4}M_{o,0}^u$, $\frac{1}{2}M_{o,0}^u$, $\frac{1}{4}M_{o,0}^u$, and 0. I then determine the corresponding $M_{o,1}$ values. I calculate $M_{r,0}$ and $M_{r,1}$ similarly.

Appendix B: Life History Simulator Salmon Final Condition Details

I choose 18 final conditions for the reconstruction in order to test the sensitivity of the assessment to this condition:

- *True*: use the true at-sea population values by total age to establish a base case (although unknown in the natural world (Pickett et al., 2007; Raymo, 1991); best-case scenario).
- *Zero*: use 0 across the ages, as done in Mohr (2006b).
- *Iterative*: use the $\hat{A}(a, 1)$ values derived by using *Zero* as the final condition, then use the $\hat{A}(a, 1)$ from this reconstruction run as the final condition for the next run, repeat this process until $\hat{A}(a, 1) = \hat{A}(a, T)$.
- *Uniform*: for the remaining cases, I first specify the total of the final condition, $\sum_{a=2}^{7} \hat{A}(a, T + 1) = A^*$ where $A^* = 10000, 20000, ..., 50000$. For the *Uniform* case, I distribute A^* uniformly, so $\hat{A}(a, T + 1) = \frac{A^*}{6}$.

- *Forward*: use the distribution of the total yield by age to find the proportion of fish of age a caught, $p(a) = \frac{Y(a)}{\sum_{a=2}^{7} Y(a)}$, and then distribute A^* by $\hat{A}(a, T+1) = p(a) \cdot A^*$.
- *Backward*: use the reverse distribution of that used for *Forward*. For instance, if w finI $p(a) = 0.6, 0.2, 0.09, 0.06, 0.04, 0.01$ for ages $2, 3, 4, 5, 6, 7$, respectively, then I apply the proportion 0.01 for age 2, 0.04 for age 3, and so forth.

Appendix C: Life History Simulator Salmon Result Details

In Figure 28 I show the at-sea population dynamics for the $M^*(3)$ case, however the results are qualitatively similar for the remaining simulation runs. The dynamics are run to steady state, and then fishing is implemented for 20 years. After fishing stops, the population recovers to its previous unfished level.

Regardless of the natural mortality rate used, after six iterations the final condition does not influence the results due to the iterative and discrete nature of the reconstruction; this means that from time step 15 and earlier, the results are identical for the 18 final conditions for a particular natural mortality rate. The reason for this result becomes clear when we consider Figure 5. The influence of the final condition, for each age, $\hat{A}(a, T+1)$ propagates diagonally, upward and to the left. From this, we see that $\hat{A}(7, T+1)$ is the most influential term, however this contribution is lost by the 6th time step backwards (t=15). In Figure 29 I depict the number of at-sea fish for all 18 final conditions (see Appendix B), for both the final time step ($t = 21$) and the time step where the results have converged ($t = 15$). These results are for the $M^*(3)$ scenario, but the remaining natural mortality scenarios are nearly identical and all converge at time step 15. These results do not change when considering the time series without the first five years of data since this is a backward iterating process and

removing these data points does not influence time $t = 6$ or later.

Using the results for the $M^*(3)$ scenario, I plot the true (simulated) ocean abundance by age and year against the estimated ocean abundance by corresponding age and year, for each final condition, in Figure 30. These results are qualitatively similar for the other natural mortality scenarios; the vast majority of the points fall above the line in the figure, and thus the assessment is overestimating the simulated population. I also note that the *Uniform* and *Backward* scenarios overestimate the simulated population more than the other final condition scenarios. Additionally, in each plot we see three or four distinct clumps of points; these clusters are created by the different ages. For instance, the far right cluster is composed of age 2 fish over the years, the second most right clump is made up of age 3 fish, and so on. Age $5, 6$, and 7 fish are located at the left most side of the graph and tend to overlap. These results change very little for the shorter time series.

To quantitatively compare between the results for the various final conditions I compute the average absolute bias $\bar{\phi}$ (Equation 19) for each final condition, for each natural mortality scenario, resulting in $\bar{\phi}_{M^*(i)}$ (Table 6). From this I find that the average absolute bias for each natural mortality scenario, across the final conditions, is smaller than the successive bias value (i.e., $\bar{\phi}_{M^*(1)} < \bar{\phi}_{M^*(2)} < \bar{\phi}_{M^*(3)} < \bar{\phi}_{M^*(4)} < \bar{\phi}_{M^*(5)}$), for each final condition. This result is intuitive, since as the natural mortality within the simulator becomes more size-dependent it differs more from the natural mortality used in the assessment. I expect the results to become more dissimilar across the final conditions. Also, for natural mortality scenarios $M^*(2)$ through $M^*(5)$ the order of the average absolute bias from minimum to maximum, according to final condition, is *Zero*, *Forward 10000*, *True*, *Iterative*, *Forward 20000*, *Forward 30000*, *Forward 40000*, *Forward 50000*, *Backward 10000*, *Uniform 10000*, *Backward 20000*, *Backward 30000*, *Uniform 20000*, *Backward 40000*, *Backward 50000*, *Uniform 30000*, *Uniform 40000*, *Uniform 50000*. However, for the $M^*(1)$ scenario the results are the same, with the exception of *Backward 30000* and *Uniform 20000*, which are switched. I would

expect the *Forward* scenarios to outperform the *Backward* scenarios, since the *Backward* scenarios place an over abundance of fish in the older age classes. Since the older age classes propagate for longer in the reconstruction than the younger age classes, this overestimate increases estimates more dramatically. It is interesting to note that the *Uniform* scenarios do the worst overall, while the *Zero* scenario produces the smallest average absolute bias. This makes sense if the overall reconstruction tends to overestimate the true population, then starting with no additional fish in the final time step will help to mitigate this effect and even out perform the *True* scenario.

Appendix D: Quota-Effort Alternative Effort-Harvest Relationships

Consider a non-linear effort-harvest relationship, where b_0 and b_1 are parameters that dictate this relationship. Let total mortality be $Z_i = M + q_i \cdot E^{b_1}$. Then harvest is

$$H_i(t) = \frac{q_i \cdot E^{b_1}}{Z_i} \cdot (1 - e^{-Z_i}) \cdot A_i(t)^{b_0}, \tag{D1}$$

where b_0 represents the possible changes in catchability with stock size. If $b_1 = 1$, then $b_0 < 1$ represent hyperstability in the catch per effort, $b_0 = 1$ represents proportionality (this is the scenario used in the current implementation), and $b_0 > 1$ represents hyperdepletion (Walters and Martell, 2004). The b_1 parameter allows additional flexibility within the relationship.

Using this effort-harvest relationship, the harvest rate is

$$h.r_i(t) = \frac{H_i(t)}{A_i(t)} = \frac{q_i \cdot E^{b_1}}{Z_i} \cdot (1 - e^{-Z_i}) \cdot A_i(t)^{b_0 - 1}. \tag{D2}$$

And the harvest rate per unit effort is

$$h.r.f_i(t) = \frac{h.r_i(t)}{E} = \frac{q_i \cdot E^{b_1 - 1}}{Z_i} \cdot (1 - e^{-Z_i}) \cdot A_i(t)^{b_0 - 1}. \tag{D3}$$

Then, the calculation to determine effort becomes

$$f_i(t) = \frac{H_i(t)}{A_i(t) \cdot h.r.f_i(t)} = \frac{\frac{q_i \cdot E^{b_1}}{Z_i} \cdot (1 - e^{-Z_i}) \cdot A_i(t)^{b_0}}{A_i(t) \cdot \frac{q_i \cdot E^{b_1 - 1}}{Z_i} \cdot (1 - e^{-Z_i}) \cdot A_i(t)^{b_0 - 1}} \tag{D4}$$

$$= \frac{E^{b_1} \cdot A_i(t)^{b_0}}{E^{b_1 - 1} \cdot A_i(t)^{b_0}} = E. \tag{D5}$$

Therefore, regardless of the effort-harvest relationship, the calculation for determining effort regains the true effort value when no uncertainty is present in the inputs to the calculation.

References

Aguirre, A. A., S. C. Gardner, J. C. Marsh, S. G. Delgado, C. J. Limpus, and W. J. Nichols (2006). Hazards associated with the consumption of sea turtle meat and eggs: a review for health care workers and the general public. *EcoHealth 3*(3), 141–153.

Bergeron, J. M., D. Crews, and J. A. McLachlan (1994). PCBs as environmental estrogens: turtle sex determination as biomarker of environmental contamination. *Environ. Health Perspec. 102*(9), 780–781.

Beverton, R. J. H. and S. J. Holt (1957). *On the Dynamics of Exploited Fish Populations*. Chapman & Hall, London, UK.

Bjorndal, K. A., A. B. Bolten, and M. Y. Chaloupka (2003). Survival probability estimates for immature green turtles *Chelonia mydas* in the Bahamas. *Marine Ecology Progress Series 252*, 273–281.

Boehlert, G. W. and R. F. Kappenman (1980). Variation of growth with latitude in two species of rockfish (*Sebastes pinniger* and *S. diploproa*) from the northeast Pacific ocean. *Marine Ecology - Progress Series 3*, 1–10.

Bonier, F., P. R. Martin, I. T. Moore, and J. C. Wingfield (2009). Do baseline glucocorticoids predict fitness? *Trends in Eco. and Evo. 24*(11), 634–642.

Breuner, C. W., S. H. Patterson, and T. P. Hahn (2008). In search of relationships between the acute adrenocortical response and fitness. *General and Comp. Endocrin. 157*(3), 228–295.

Brooks, E. N., J. E. Powers, and E. Cortés (2010). Analytical reference points for age-structured models: Application to data-poor fisheries. *ICES Journal of Marine Science 67*(1), 165–175.

Brown, V. and D. Hively (2011). Assessing the assessments: A life history simulator to test stock assessment models and methods. *Natural Resource Modeling* (submitted).

Chen, Y., L. Chen, and K. I. Stergious (2003). Impacts of data quantity on fisheries stock assessment. *Aquatic Sciences 65*(1), 92–98.

Clark, C. W. and M. Mangel (2000). *Dynamic State Variable Models in Ecology: Methods and Applications*. Oxford University Press, New York, NY, USA.

de Valpine, P. and R. Hilborn (2005). State-space likelihoods for nonlinear fisheries time-series. *Can. J. Fish. Aquat. Sci. 62*(9), 1937–1952.

Feller, W. (1971). *An Introduction to Probability Theory and Its Applications Volume II*. John Wiley and Sons, New York, NY, USA.

Forbes, V. E. and P. Calow (1996). Costs of living with contaminants: implications for assessing low-level exposures. *Biological Effects of Low Level Exposures Newsletter 4*(3), 1–8.

Groot, C. and L. Margolis (1991). *Pacific Salmon Life Histories*. UBC Press, Vancouver, British Columbia, Canada.

Gulland, J. (Ed.) (1988). *Fish Population Dynamics: The Implications for Management* (2*nd* ed.). John Wiley & Sons Ltd., London, UK.

Haldorson, L. and M. Love (1990). Maturity and fecundity in the rockfishes, *Sebastes* spp., a review. *Marine Fisheries Review 53*(2), 25–31.

Hilborn, R. and M. Mangel (1997). *The Ecological Detective: Confronting Models with Data*. Princeton University Press, Princeton, New Jersey, USA.

Jennings, S., M. J. Kaiser, and J. D. Reynolds (2001). *Marine Fisheries Ecology*. Blackwell Science, Oxford, London.

Koch, V., L. B. Brooks, and W. J. Nichols (2007). Population ecology of the green/black turtle (*Chelonia mydas*) in Bahía Magdalena, Mexico. *Marine Biology 153*(1), 35–46.

Koch, V., W. J. Nichols, H. Peckham, and V. de la Toba (2006). Estimates of sea turtle mortality from poaching and bycatch in Bahía Magdalena, Baja California Sur, Mexico. *Biological Conservation 128*(3), 327–334.

Labrada-Martagón, V., L. C. Méndez-Rodríguez, S. C. Gardner, V. H. Cruz-Escalona, and T. Zenteno-Savín (2010b). Health indices of the green turtle (*Chelonia mydas*) along the Pacific coast of Baja California Sur, Mexico. II. Body condition index. *Chelonian Cons. and Bio. 9*(2), 173–183.

Labrada-Martagón, V., L. C. Méndez-Rodríguez, S. C. Gardner, M. López-Castro, and T. Zenteno-Savín (2010a). Health indices of the green turtle (*Chelonia mydas*) along the Pacific coast of Baja California Sur, Mexico. I. Blood biochemistry values. *Chelonian Cons. and Bio. 9*(2), 162–172.

Labrada-Martagón, V., P. A. Tenorio-Rodríguez, L. C. Méndez-Rodríguez, and T. Zenteno-Savín (2011). Oxidative stress indicators and chemical contaminants in East Pacific green turtles (*Chelonia mydas*) inhabiting two foraging coastal lagoons in the Baja California peninsula. *Compar. Biochem. and Phys. Part C: Toxicology and Pharmacology 154*(2), 65–75.

Lorenzen, K. (1996). The relationship between body weight and natural mortality in juvenile and adult fish: A comparison of natural ecosystems and aquaculture. *Journal of Fish Biology 49*, 627–647.

Ludwig, D. and C. J. Walters (1985). Are age-structured models appropriate for catch-effort data? *Can. J. Fish. Aquat. Sci. 42*(6), 1066–1072.

Lutz, P. L. and J. A. Musick (Eds.) (1997). *The Biology of Sea Turtles*. CRC Press, Boca Raton, Florida, USA.

Lutz, P. L., J. A. Musick, and J. Wyneken (Eds.) (2003). *The Biology of Sea Turtles, Volume II*. CRC Press, Boca Raton, Florida, USA.

Mangel, M., J. Brodziak, and G. DiNardo (2010). Reproductive ecology and scientific inference of steepness: A fundamental metric of population dynamics and strategic fisheries management. *Fish and Fisheries 11*(1), 89–104.

Mangel, M. and C. W. Clark (1988). *Dynamic Modeling in Behavioral Ecology*. Princeton University Press, Princeton, NJ, USA.

McElhany, P., E. A. Steel, K. Avery, N. Yoder, C. Busack, and B. Thompson (2010). Dealing with uncertainty in ecosystem models: Lessons from a complex salmon model. *Ecological Applications 20*(2), 465–482.

Mohr, M. S. (2006b). The cohort reconstruction model for Kalamath River fall Chinook salmon. Unpublished report. National Marine Fisheries Service, Santa Cruz, CA.

Pickett, S. T. A., J. Kolasa, and C. G. Jones (2007). *Ecological Understanding: The Nature of Theory and the Theory of Nature*. Academic Press, Amsterdam.

Post, J. R. and D. O. Evans (1989). Size-dependent overwinter mortality of young-of-the-year yellow perch (perca flavescens): Laboratory, in situ enclosure, and field experiments. *Can. J. Fish. Aquat. Sci. 46*, 1958–1968.

Quinn, T. P. (2005). *The Behavior and Ecology of Pacific Salmon and Trout*. University of Washington Press, Seattle, Washington, USA.

Raymo, C. (1991). *The Virgin and the Mousetrap: Essays in Search of the Soul of Science*. Viking, New York.

Ricker, W. (1958). Handbook of computations for biological statistics of fish populations. *Bull. Fish. Res. Board. Can. 119*, 1–300.

Roff, D. A. (1992). *The Evolution of Life Histories: Theory and Analysis*. Chapman and Hall, New York, NY, USA.

Rose, K. A. and J. H. Cowan, Jr. (2003). Data, models, and decisions in U.S. marine fisheries management: Lessons for ecologists. *Annu. Rev. Ecol. Evol. Syst. 34*, 127–151.

Stearns, S. C. (1992). *The Evolution of Life Histories*. Oxford University Press, Oxford, UK.

Vicens, Q. and P. E. Bourne (2007). Ten simple rules for a successful collaboration. *PLoS Computational Biology 3*(3), e44.

von Bertalanffy, L. (1957). Quantitative laws in metabolism and growth. *Quarterly Review of Biology 32*(3), 217–231.

Walters, C. J. and S. J. D. Martell (2004). *Fisheries Ecology and Management*. Princeton University Press, Princeton, NJ, USA.

Wang, S.-P., M. N. Maunder, and A. Aires-da-Silva (2009). Implications of model and data assumptions: An illustration including data for the Taiwanese longline fishery into the eastern Pacific Ocean bigeye tuna (*Thunnus obesus*) stock assessment. *Fisheries Research 97*(1-2), 118–126.

Wetzel, C. R. and A. E. Punt (2011). Model performance for the determination of appropriate harvest levels in the case of data-poor stocks. *Fisheries Research 110*(2), 342–355.

Table 1: Parameters used in Chinook salmon life history simulator.

Variables	Interpretation
a_r, a_o, a_T	River age, ocean age, and total age
$a_{r,max}, a_{o,max}$	Maximum river age and maximum ocean age
i, n	River, total number of rivers
M_o, M_r	Natural ocean mortality and natural river mortality
$M_{r,0}, M_{r,1}, M_{o,0}, M_{o,1}$	Natural mortality parameters
$M^*(1), M^*(2), M^*(3), M^*(4), M^*(5)$	5 natural mortality pairs describing the proportion of natural mortality that is size-dependent and size-independent
M_{oe}	Ocean entry mortality
M_{re}	River return mortality
$\mathcal{F}$	Fishing mortality
L_r, L_o	Length at river age, length at ocean age
$L_\infty, k, \tau_0, L_{o,\infty}, k_o$	von Bertalanffy growth parameters
$h(i)$	Proportion of fish born in river i that return home to spawn
$g(i)$	Proportion of parr from natal river i that go to the ocean
β, γ	Ricker density dependence and Ricker parameter
K_{fm}	Number of females one male can fertilize
$b(i', i)$	Probability that an individual born in river i' returns to river i to spawn
$\alpha(i', i)$	Maximum reproductive ability of a spawner from natal river i' that returned to current river i to spawn
δ	Gonadosomatic index
A	At-sea life history stage
S_T	Total spawners
E_T	Total eggs
w_E	Egg mass
ρ	Fraction of eggs fertilized
P	Parr life history stage
Y	Yield

Table 2: Model assumptions for the Chinook salmon life history simulator and assessment problem.

Simulator	Stock Assessment
Size-dependent natural mortality (5 levels)	Constant natural mortality
At-sea (ocean), spawner, egg, and parr stages are modeled	Only ocean abundance is modeled
Length at age is calculated	Length at age is not calculated
Number of fish tracked by river and ocean age, time, location	Abundance tracked by total age and time

Table 3: Details for the SRFC & KRFC data for the quota-effort problem.

Data	SRFC	KRFC
Harvest Rates	not age specific	age specific
Abundance	updated annually, not age specific, index of abundance	updated monthly, age specific, estimate of abundance

Table 4: Model parameters for the green sea turtle problem.

Parameter	Value
Size at maturity	77.3 cm
$log(a)$	PAO: -8.7; BMA: -7.947
b	PAO: 2.96; BMA: 2.77
weight (kg)	PAO: 2.29 3.93 6.20 9.20 13.04 17.81 23.61 30.55 38.71 48.21 59.13 71.58
	BMA: 2.64 4.37 6.70 9.69 13.43 17.99 23.42 29.80 37.20 45.68 55.30 66.13
mature weight	PAO: 64.66; BMA: 60.13
damage levels	0 to 20

Table 5: Comparison of juvenile green sea turtle survival rates in the model and from a physical system.

Time t	# of indiv. that mature at time t	# of indiv. that mature at time t/50	0.761^t
4	21	0.42	0.335
5	12	0.24	0.255
6	14	0.28	0.194
7	7	0.14	0.148
8	5	0.10	0.112
9	3	0.06	0.086
10	4	0.08	0.065
12	1	0.02	0.038
14	2	0.04	0.022

Table 6: Bias in abundance estimates across final conditions for the cohort reconstruction and simulation mortality scenarios for the Chinook salmon life history simulation problem.

Final Condition	$M^*(1)$	$M^*(2)$	$M^*(3)$	$M^*(4)$	$M^*(5)$
True	0.1881742	0.1904654	0.1927938	0.1958953	0.1991007
Zero	0.1794604	0.1816532	0.1838828	0.1868853	0.1899937
Iterative	0.188955	0.1918986	0.1950369	0.1991611	0.2036807
Uniform 10000	0.22775	0.2313703	0.2352703	0.2402459	0.2457076
Uniform 20000	0.2387678	0.2425192	0.2465418	0.2516194	0.2571405
Uniform 30000	0.2454206	0.2491801	0.2531881	0.2582162	0.2636335
Uniform 40000	0.2500861	0.2538095	0.2577575	0.2626919	0.2679671
Uniform 50000	0.2536070	0.2572762	0.2611483	0.265977	0.2711062
Forward 10000	0.1847857	0.1876066	0.1906159	0.1945948	0.1989627
Forward 20000	0.1889620	0.1921526	0.1955923	0.2000693	0.2050183
Forward 30000	0.192378	0.1958055	0.1995090	0.204275	0.2095387
Forward 40000	0.1952551	0.1988433	0.2027191	0.2076657	0.2131147
Forward 50000	0.1977314	0.2014327	0.2054259	0.2104904	0.2160538
Backward 10000	0.2272374	0.2305239	0.2340218	0.2384879	0.2433016
Backward 20000	0.2348012	0.2381110	0.2416184	0.2460699	0.2508373
Backward 30000	0.2391477	0.2424363	0.2459112	0.2503135	0.2550117
Backward 40000	0.2421395	0.2454009	0.2488406	0.253196	0.257834
Backward 50000	0.2443926	0.2476279	0.2510355	0.2553501	0.2599377

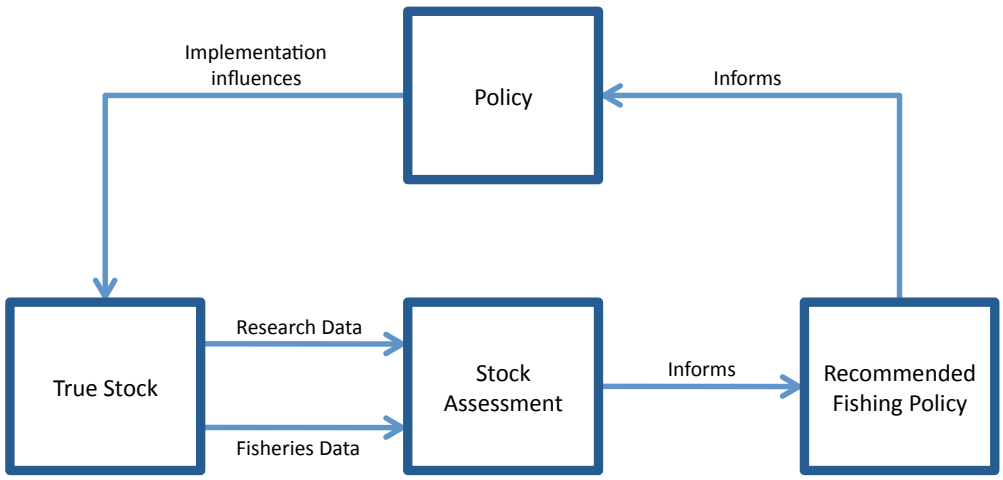

Figure 1: Both research (fisheries independent) and fisheries data may be collected for a stock and all or a subset of these data are input into a stock assessment. The results of the stock assessment can include an estimate of the abundance of the stock and are used to determine fishing regulations, which are recommended to committees, regulatory agencies, and policy makers. A policy is enacted, which in turn can influence the dynamics and status of the stock.

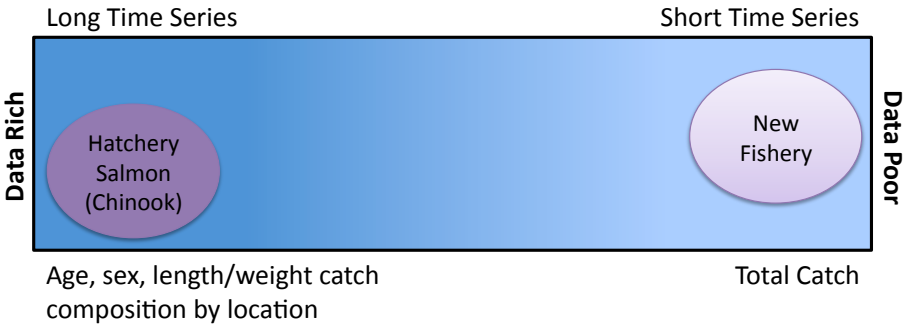

Figure 2: Data poor stocks are typically characterized by the simplest records of catch data, such as total catch in numbers or biomass over a short time series. A new fishery falls into the data poor end of the spectrum since it will necessarily have a short time series, and typically no catch composition. Alternatively, data rich stocks are often described by long time series and diverse catch compositions such as catch by age, sex, length or weight, and location. Additionally, data rich stocks can contain information pertaining to movement, mortality and growth rate, effort, and other life history parameters. Hatchery salmon, such as Chinook salmon, are typically considered data rich since recovered coded-wire-tags implanted in a proportion of these fish make it possible to reconstruct cohorts, determine distribution patterns, fishery impacts, and survival rates.

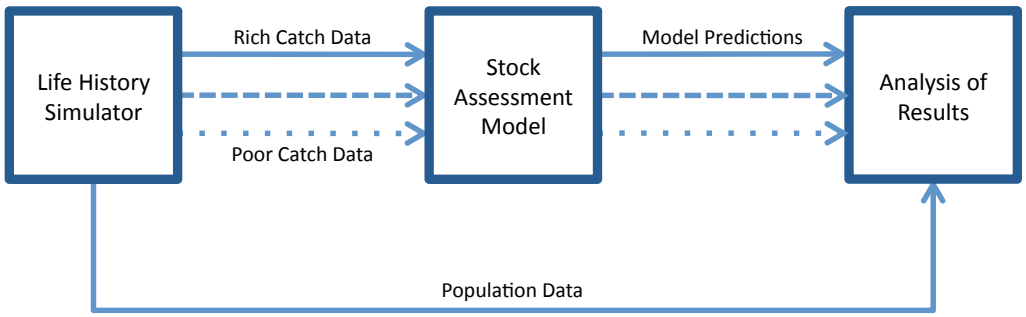

Figure 3: The life history simulator generates different levels of catch data. These are input into the stock assessment model to make predictions about the population. The results of the stock assessment for each level of data richness are compared to the complete population data from the life history simulator to determine model accuracy across increasing levels of available data.

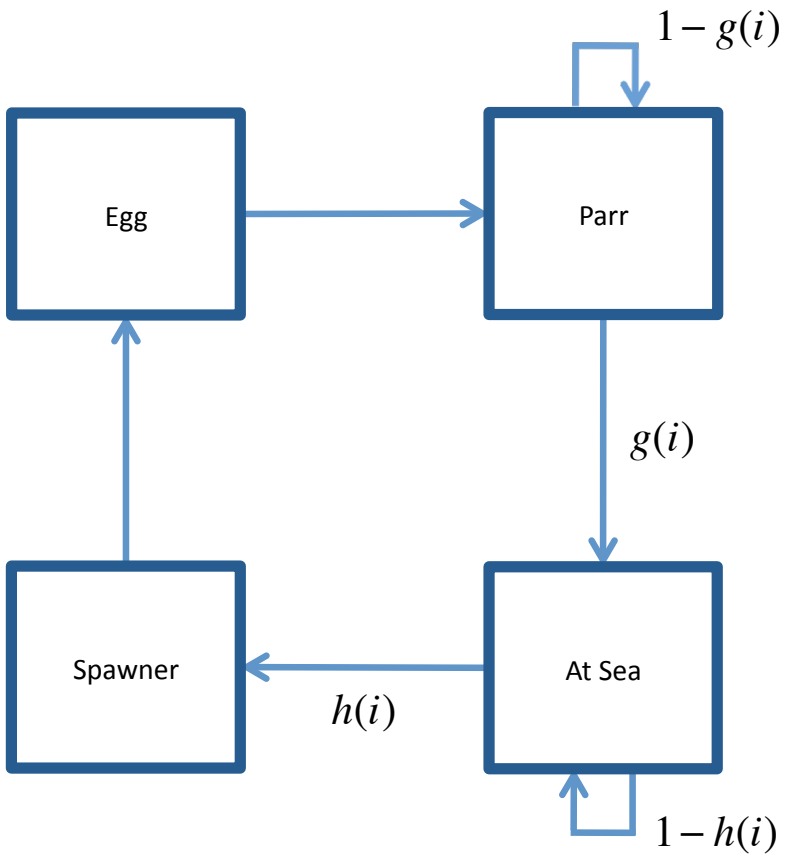

Figure 4: The four salmon life history stages explicitly modeled in the simulator. In our model, eggs transition into parr. Parr can remain in the river as parr or go (g) to the sea. The proportion of parr that remain in the river each time step is $1 - g(i)$. The remaining proportion, $g(i)$, of the parr transition to the at-sea stage. The at-sea fish can remain at-sea or return home (h) to spawn. This happens as proportions $1 - h(i)$ and $h(i)$, respectively. The spawners then produce eggs.

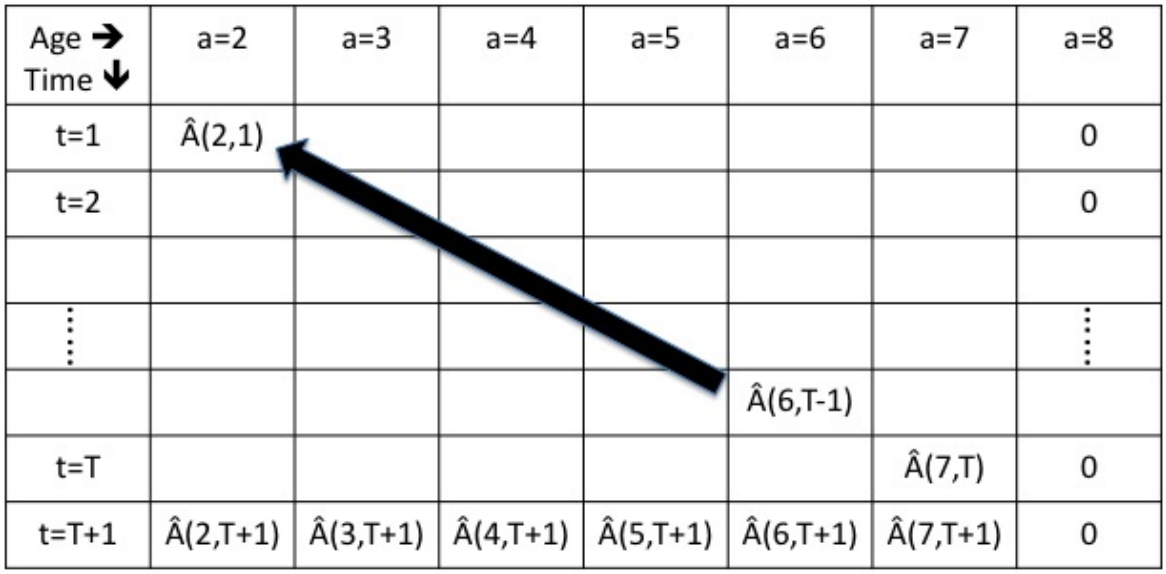

Figure 5: The estimated age-specific ocean abundance for the assessment is determined from a cohort reconstruction. This reconstruction depends on age-specific fishing and spawner data for years 1 through T, as well as a specified final condition, which is displayed in the final row of this table, at $T+1$. Due to the formulation of this reconstruction as a backward induction problem, the estimates depend on one another iteratively in a diagonal fashion from bottom to top, right to left, as depicted by the arrow.

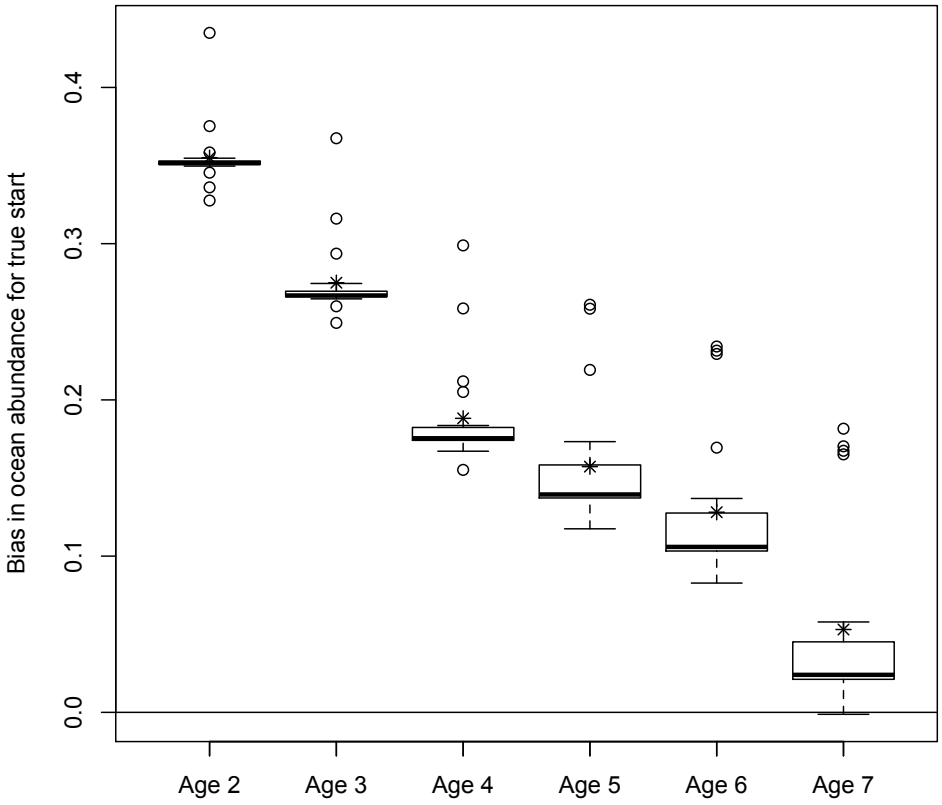

Figure 6: Bias in ocean abundance for each age, aggregating across the years. For instance, for age 2 at-sea fish, I calculate the bias for each of the twenty years of data and then perform a box plot for the bias. The thick dark line in the box plot represents the median, the star is the mean, the box is the interquartile range, the dashed lines are the range, and the circles are outliers. The horizontal line across the entire plot represents a bias of zero (i.e., the estimated population is a perfect fit to the simulated population). Values above the horizontal line indicate that the estimated population overestimates the simulated population, while values below this line represent an underestimate. These results are from the $M^*(3)$ natural mortality case.

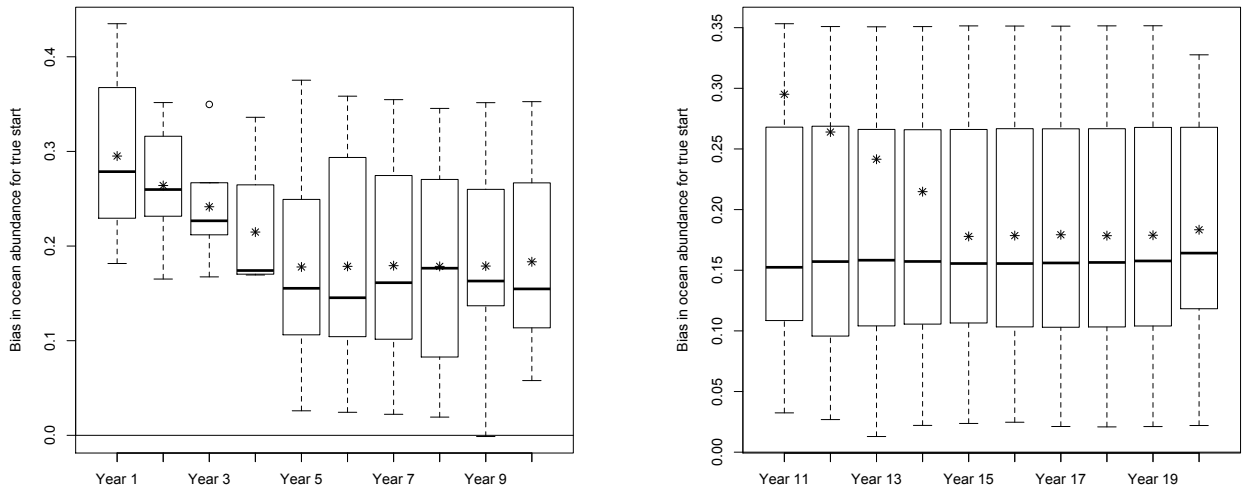

(a) Years 1-10

(b) Year 11-20

Figure 7: Bias in ocean abundance for each year, aggregating across ages. The thick dark line in the box plot represents the median, the star is the mean, the box is the interquartile range, the dashed lines are the range, and the circles are outliers. The horizontal line across the entire plot represents a bias of zero (i.e., the estimated population is a perfect fit to the simulated population). Values above the horizontal line indicate that the estimated population overestimates the simulated population, while values below this line represent an underestimate. These results are from the the $M^*(3)$ natural mortality case.

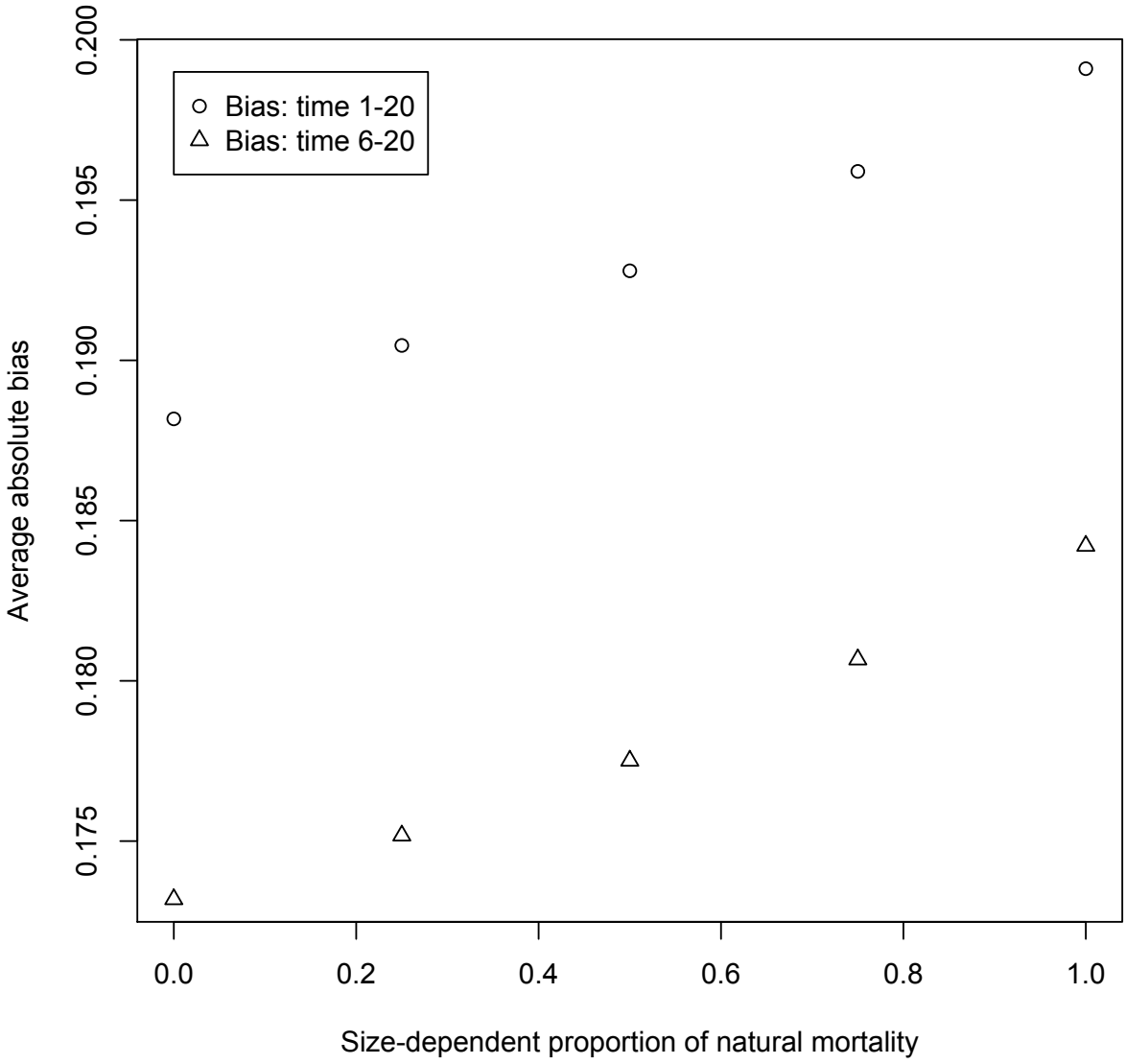

Figure 8: Absolute average bias in ocean abundance for each mortality scenario (defined by proportion of the natural mortality that is size-dependent), for the total time series (circles) as well as the after removing the first five years of data (triangles).

Image courtesy of M. O'Farrell

Figure 9: Seven ocean salmon fishery management zones off the coasts of Oregon and California. Region abbreviations: Northern Oregon (NO), Coos Bay (CO), Klamath Management Zone (KMZ) Oregon (KMZ-OR or KO), KMZ California (KMZ-CA or KC), Fort Bragg (FB), San Francisco (SF), Monterey (MO).

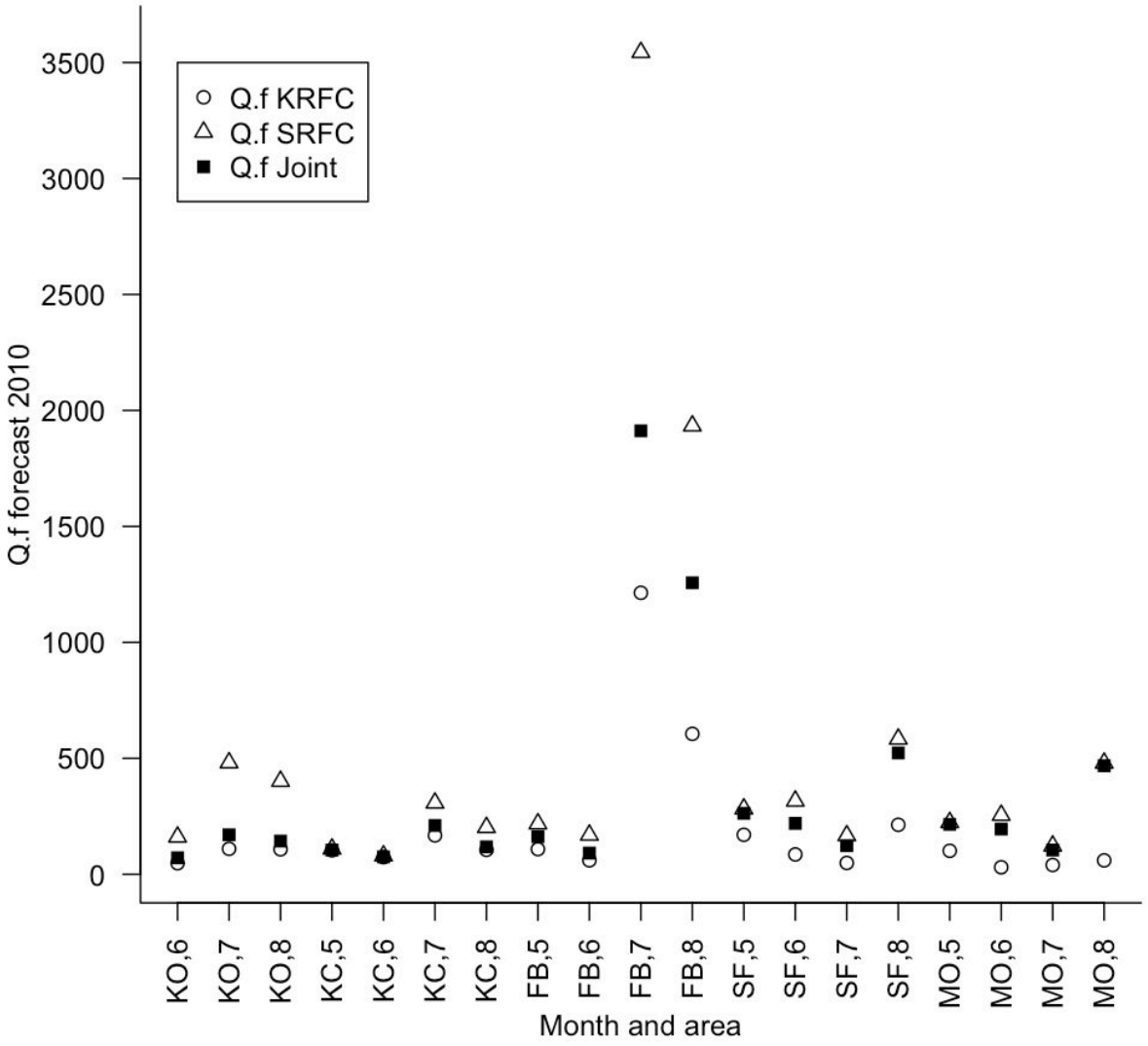

Figure 10: Area- and month-specific estimates of quota-effort (vessel days) from forecasted real data for 2010. Circles are the KRFC estimated effort values, triangles the SRFC estimated effort values, and filled squares the joint effort estimates. Recall region abbreviations: KMZ Oregon (KO), KMZ California (KC), Fort Bragg (FB), San Francisco (SF), Monterey (MO).

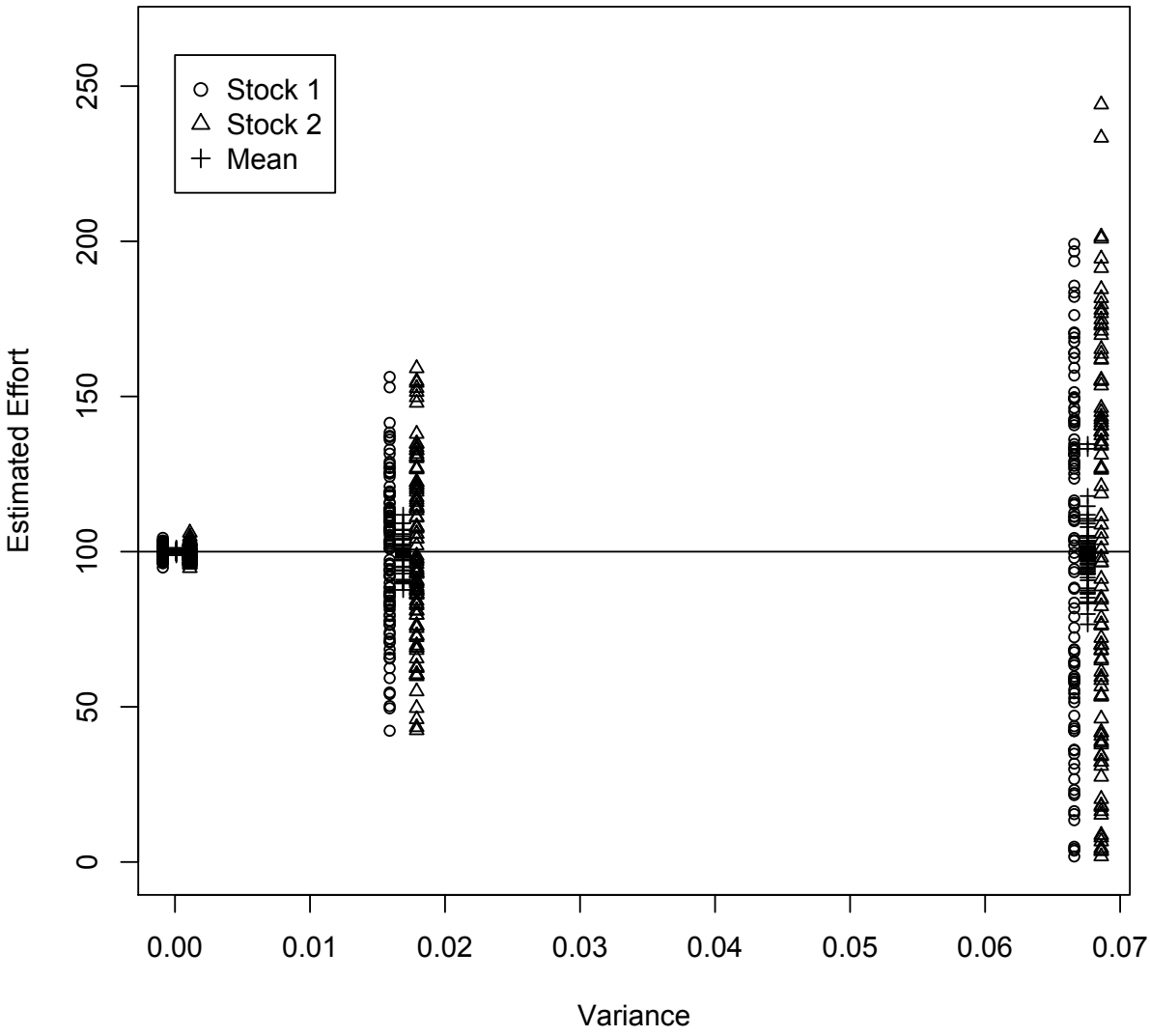

Figure 11: Stock specific effort estimates $f_1(t)$ (circles) and $f_2(t)$ (triangles), as well as the mean $f_K(t)$ (plus signs), across three variance values (left to right 0.0001, 0.0169, 0.0676) for all time. The horizontal line depicts the true effort value (as well as the estimated joint value).

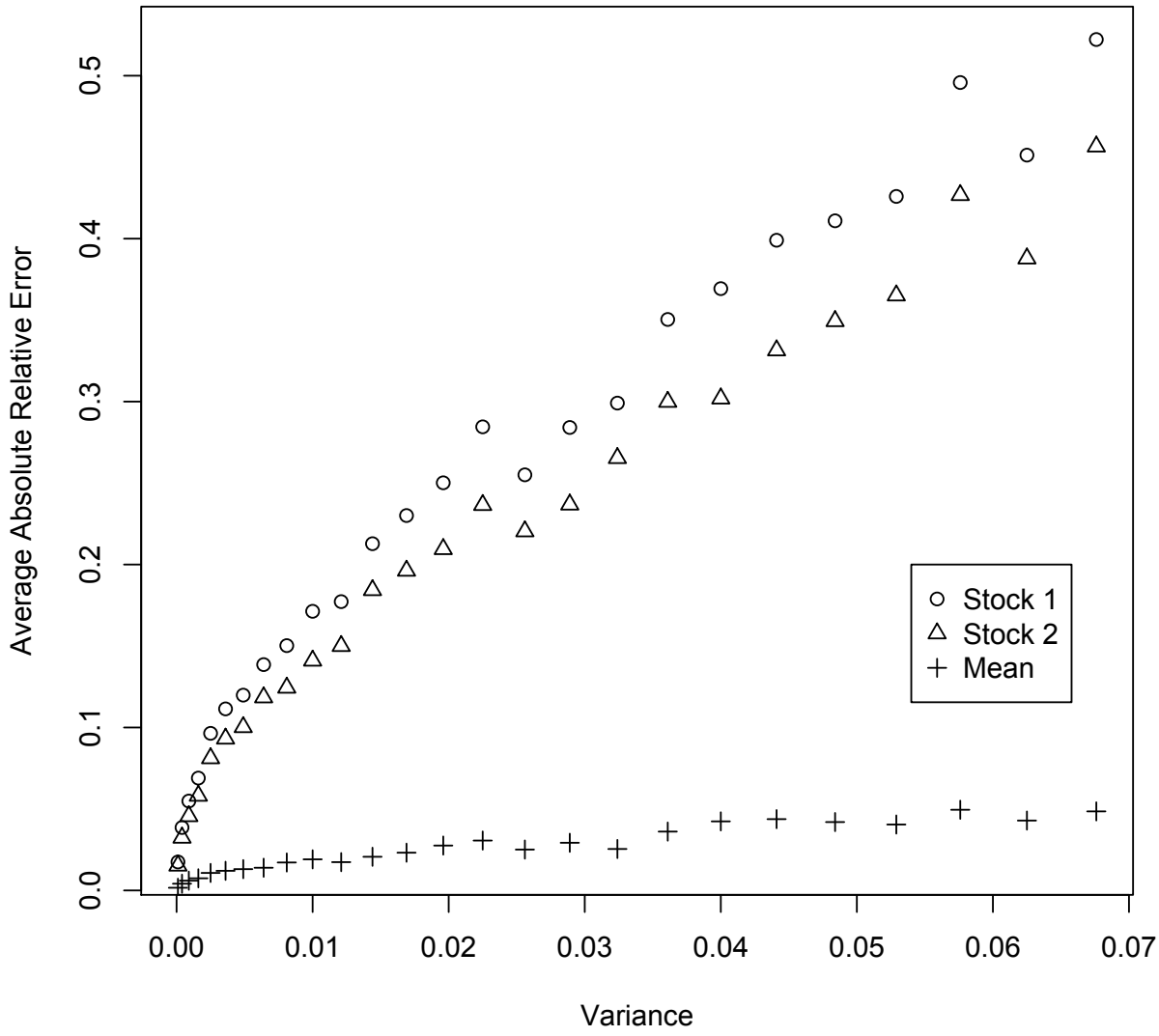

Figure 12: Stock specific average absolute relative error for effort estimates for stock 1 (circles), stock 2 (triangles), and the mean of both stock estimates (plus signs), across all the variance scenarios.

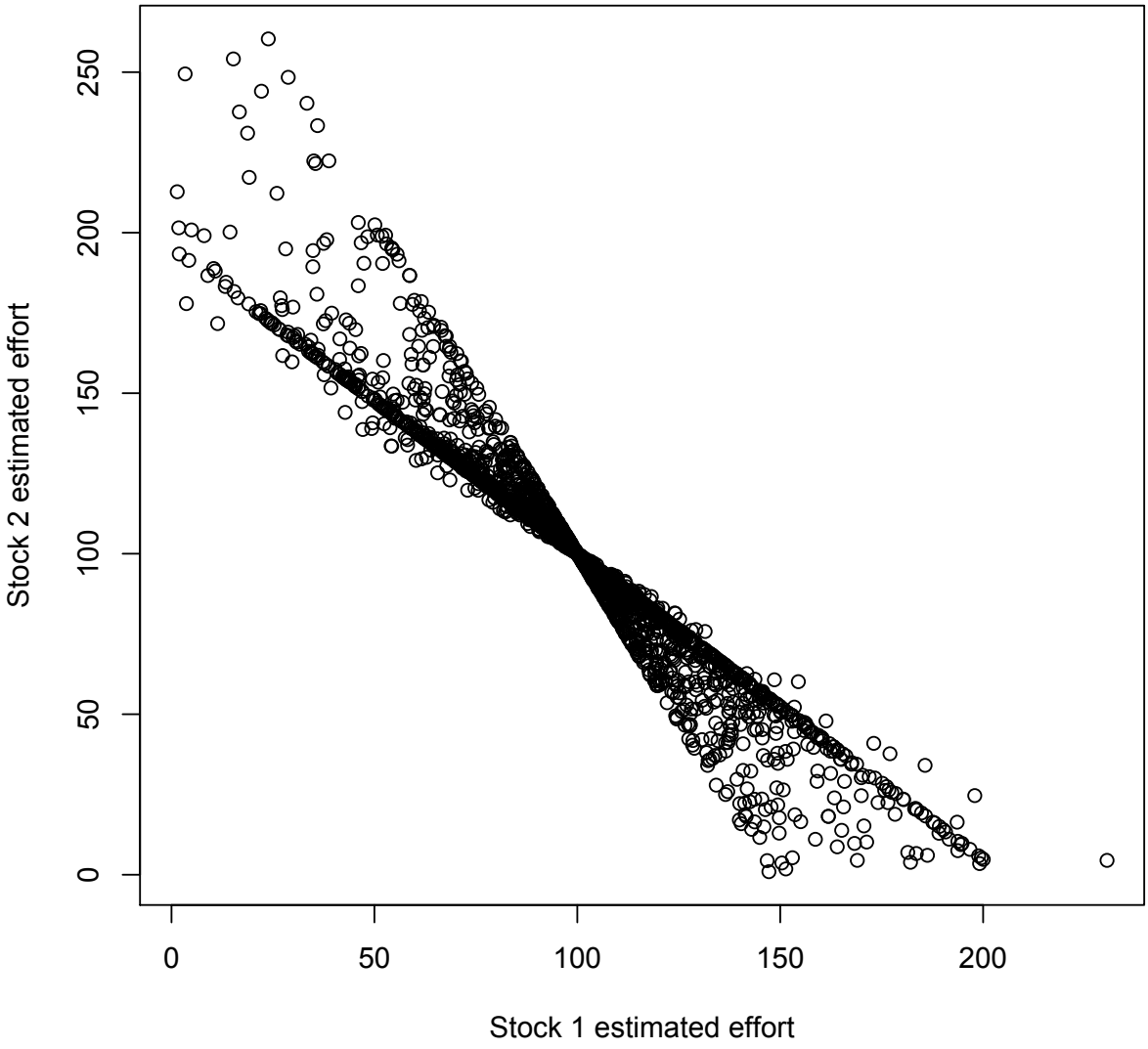

Figure 13: Effort estimates for stock 1 plotted against the effort estimates for stock 2, for each time step and variance value.

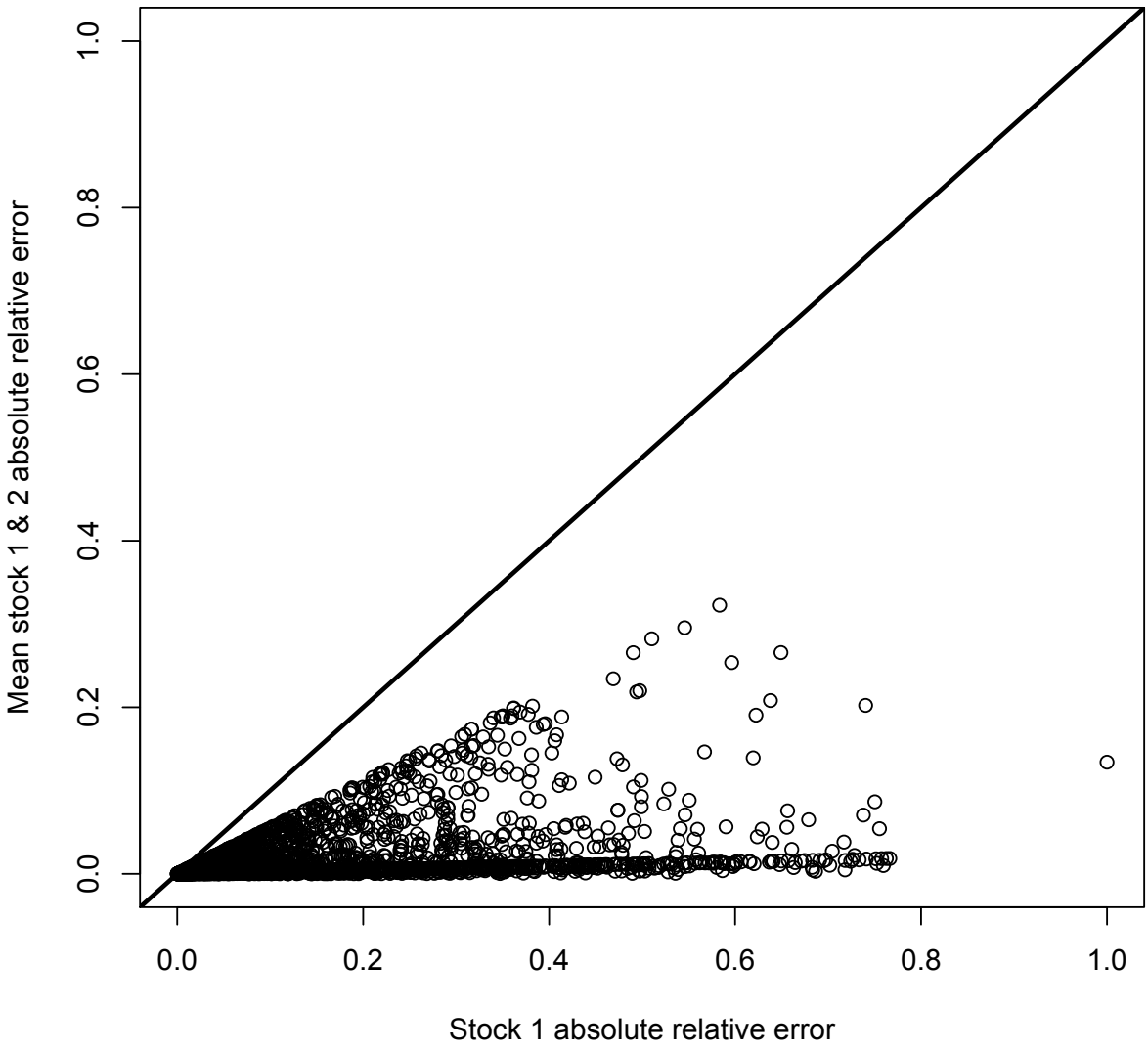

Figure 14: Absolute relative error for the effort estimates for stock 1 plotted against the absolute relative error for the effort estimates using the mean of stock 1 and 2, for each time step and variance value. The thick line represents the $y = x$ line. Points above the line indicate that the mean was less accurate than the individual estimate, points below the line indicate that the individual estimate was less accurate than the mean.

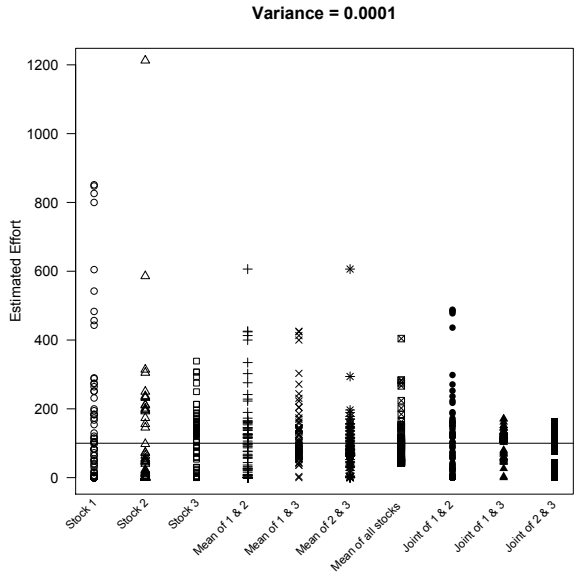

(a) $\sigma = 0.01$

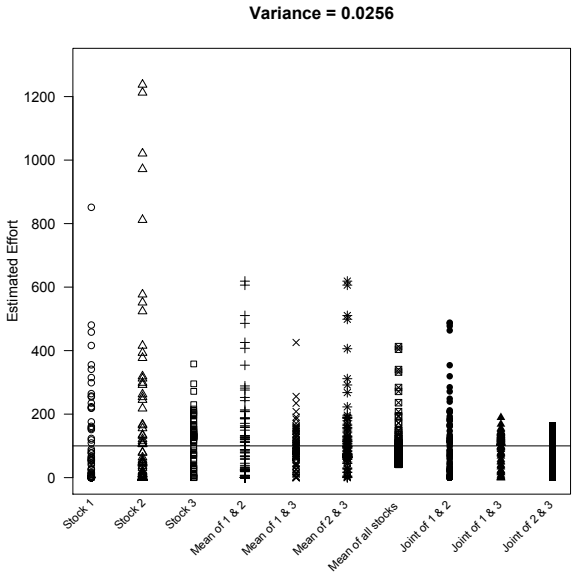

(b) $\sigma = 0.16$

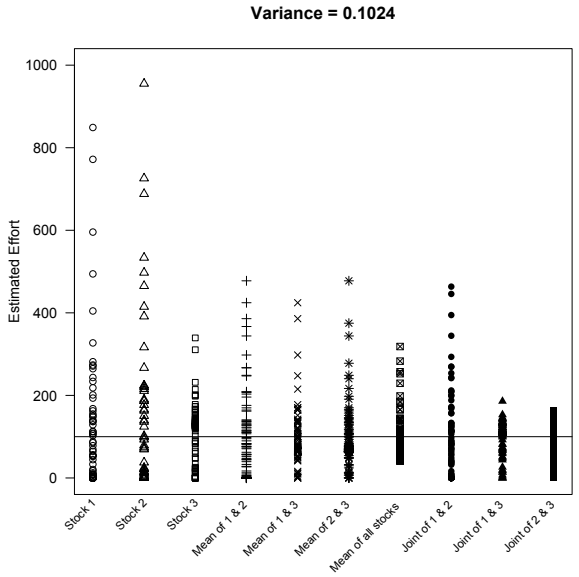

(c) $\sigma = 0.32$

Figure 15: Estimated effort for each of the ten effort calculations, for three variance values. The horizontal line in each box represents the true effort. Each symbol represents a different effort calculation type, described below the horizontal axis.

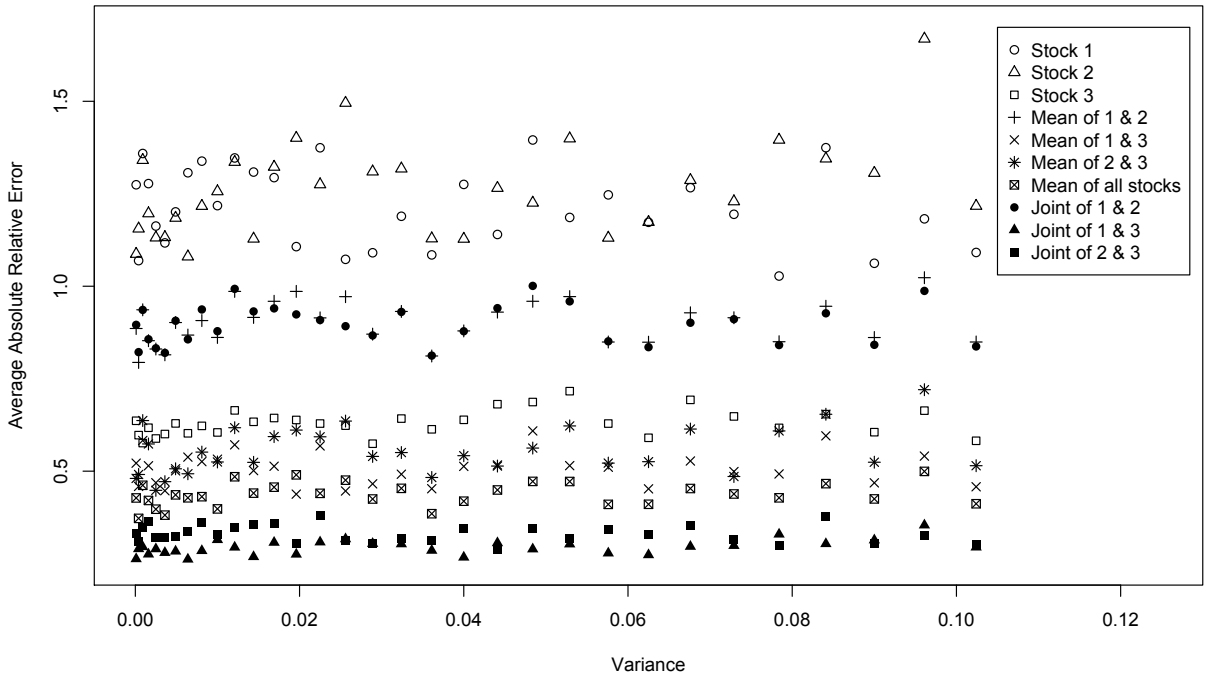

Figure 16: Average absolute relative error for each of the ten effort estimates, and each variance value. Effort estimate types: stock 1 (circles), stock 2 (triangles), stock 3 (squares), mean of stocks 1 and 2 (plus signs), mean of stocks 1 and 3 (x), mean of stocks 2 and 3 (stars), mean of all three stocks (boxes with an x inside), joint of stocks 1 and 2 (filled circles), joint of stocks 1 and 3 (filled triangles), joint of stocks 2 and 3 (filled squares).

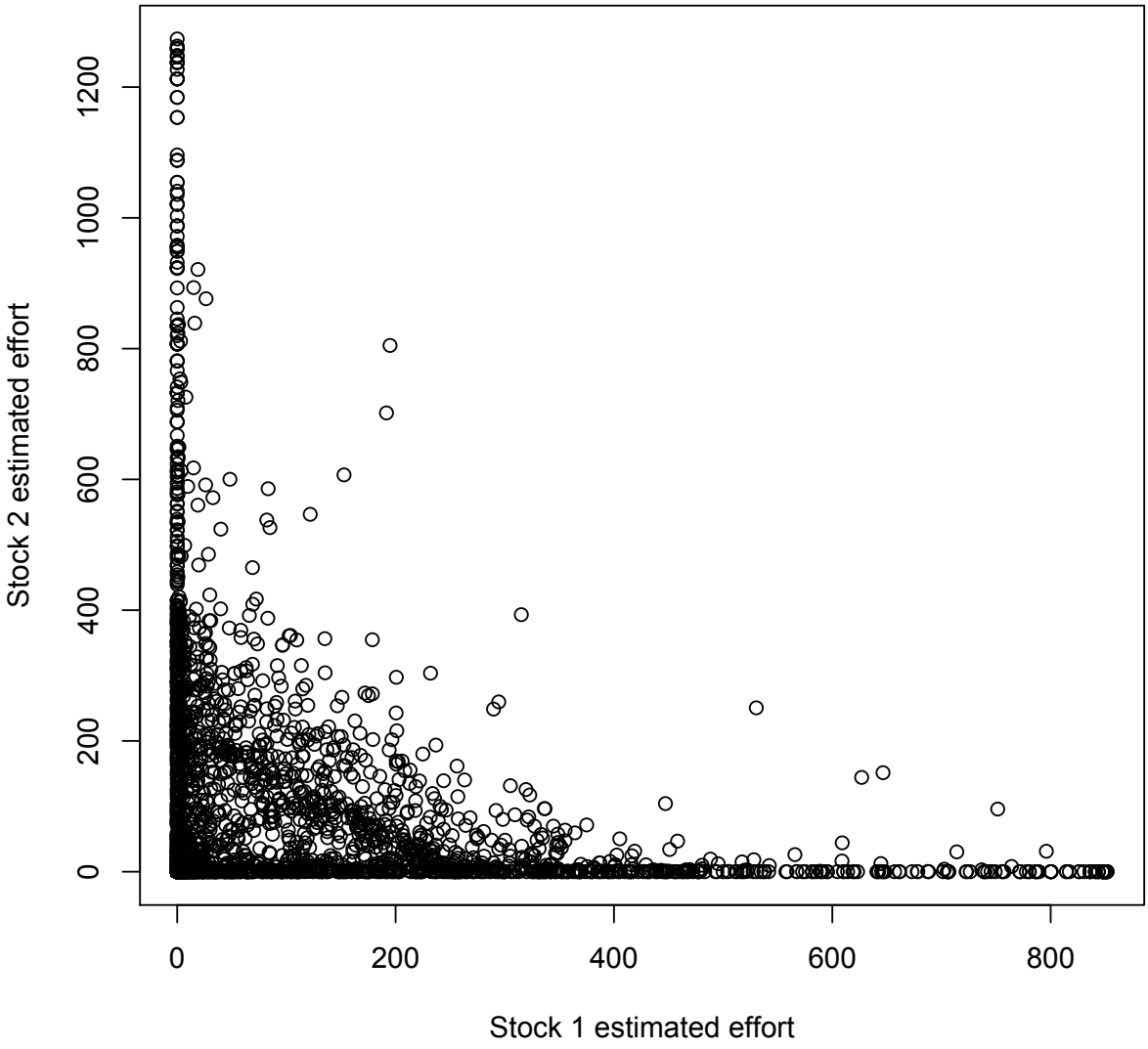

Figure 17: Effort estimates for stock 1 plotted against the effort estimates for stock 2, for each time step and variance value.

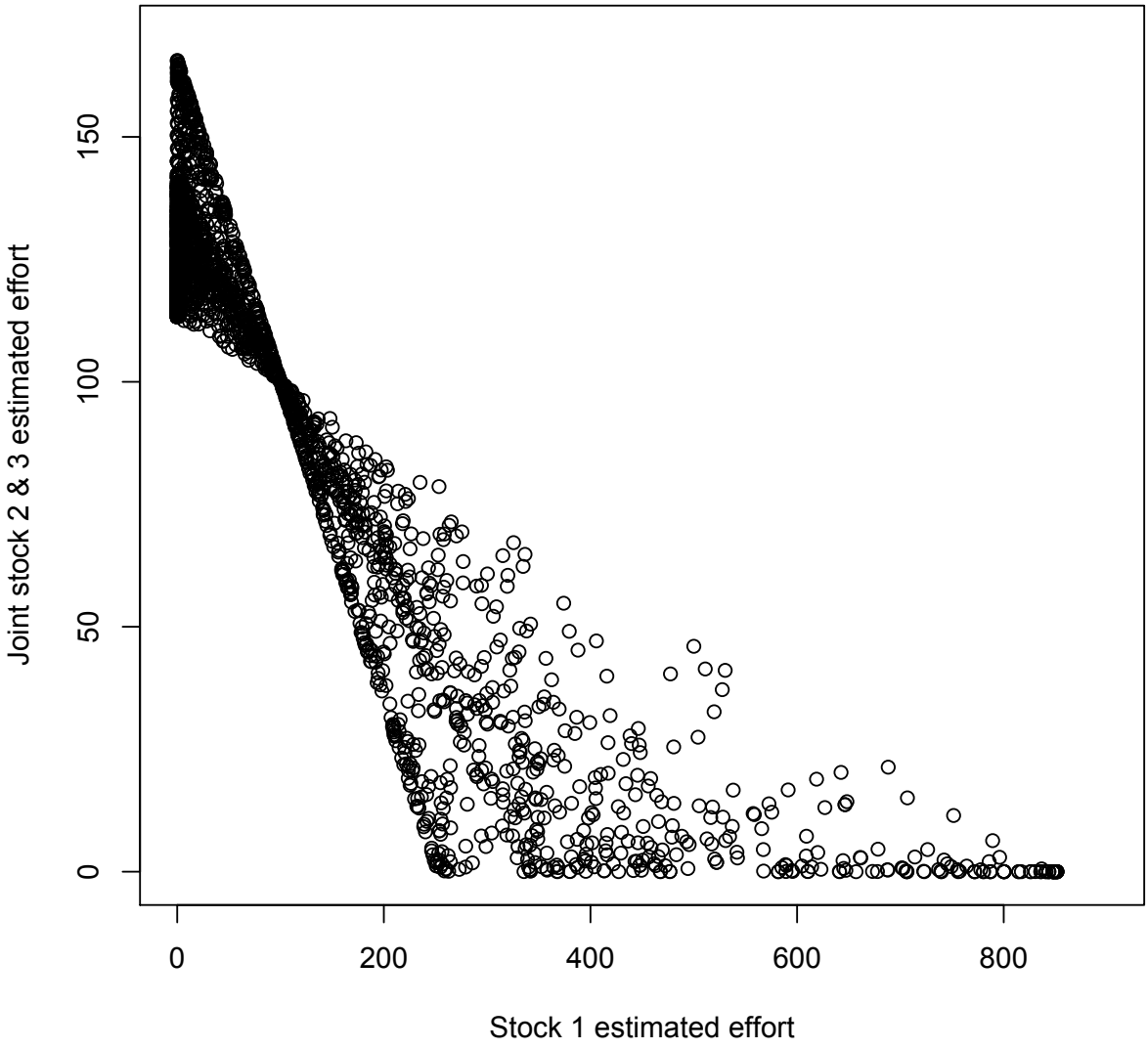

Figure 18: Effort estimates for stock 1 plotted against the joint effort estimates for stocks 2 and 3, for each time step and variance value.

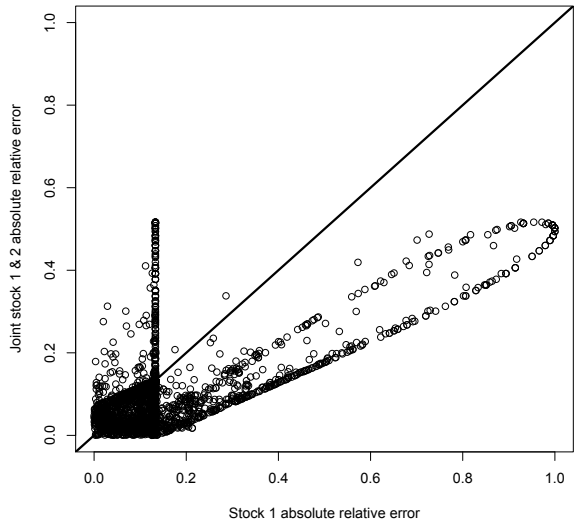

(a) Stock 1 vs. Joint stock 1 and 2

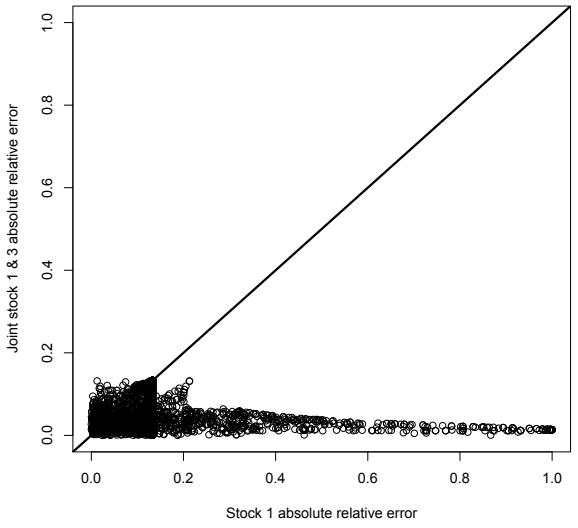

(b) Stock 1 vs. Joint stock 1 and 3

Figure 19: Absolute relative error for the effort estimates for stock 1 plotted against the absolute relative error for the effort estimates for the (a) joint of stock 1 and 2, and (b) joint of stock 1 and 3, for each time step and variance value. The thick line represents the $y = x$ line. Points above the line indicate that the joint was less accurate than the individual estimate, points below the line indicate that the individual estimate was less accurate than the joint.

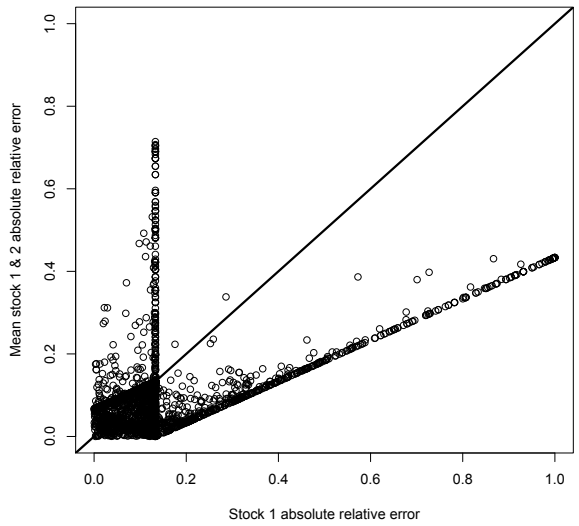

(a) Stock 1 vs. Mean stock 1 and 2

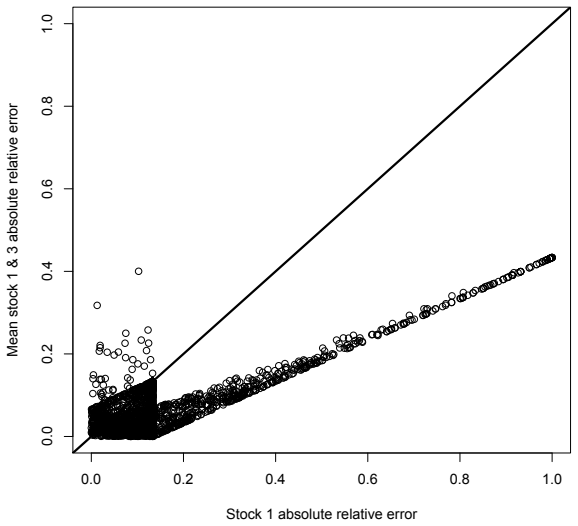

(b) Stock 1 vs. Mean stock 1 and 3

Figure 20: Absolute relative error for the effort estimates for stock 1 plotted against the absolute relative error for the effort estimates for the (a) mean of stock 1 and 2, and (b) mean of stock 1 and 3, for each time step and variance value. The thick line represents the $y = x$ line. Points above the line indicate that the mean was less accurate than the individual estimate, points below the line indicate that the individual estimate was less accurate than the mean.

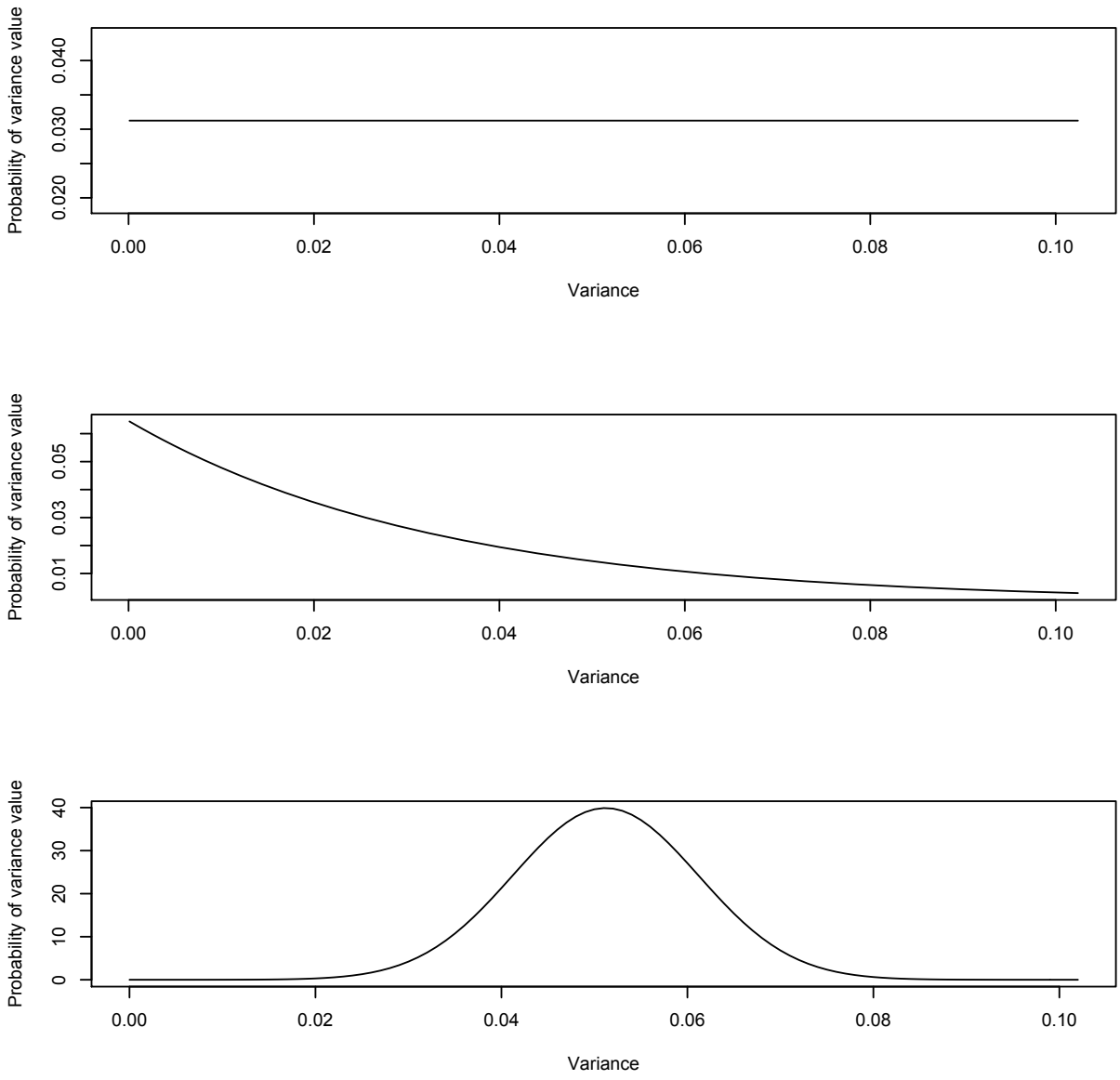

Figure 21: Possible distributions over the variance. Top graph: uniform. Middle graph: exponentially decreasing. Bottom graph: normal.

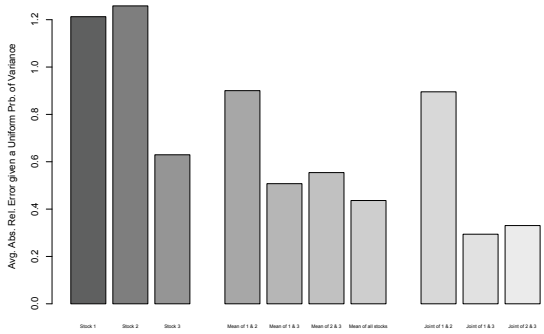

(a) Uniform variance distribution

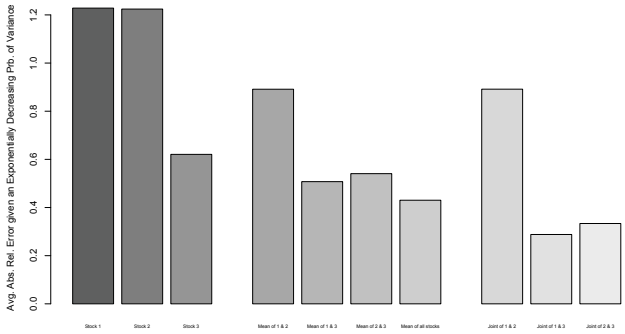

(b) Exponentially decreasing variance distribution

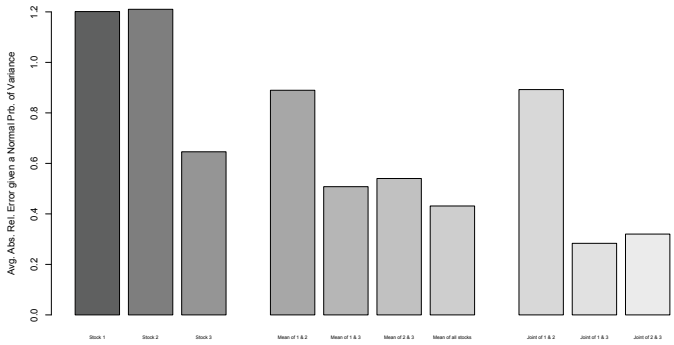

(c) Normal variance distribution

Figure 22: Weighted means of the average absolute relative errors, across three variance types, for stock 1, stock 2, stock 3, mean of 1 & 2, mean of 1 & 3, mean of 2 & 3, mean of all stocks, joint of 1 & 2, joint of 1 & 3, and joint of 2 & 3, from left to right. The corresponding variance distributions are (a) uniform, (b) exponentially decreasing, and (c) normal.

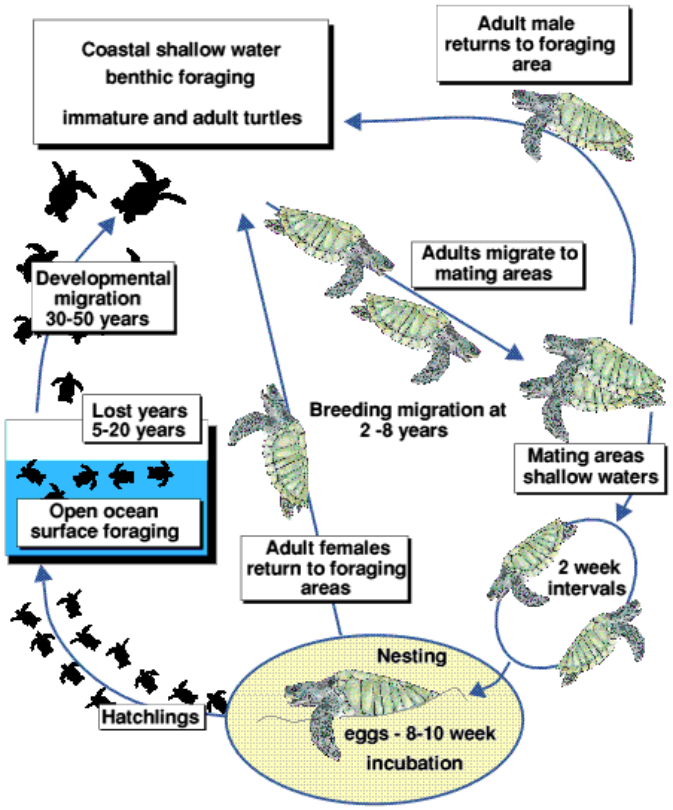

Figure 23: A general life cycle description for sea turtles.

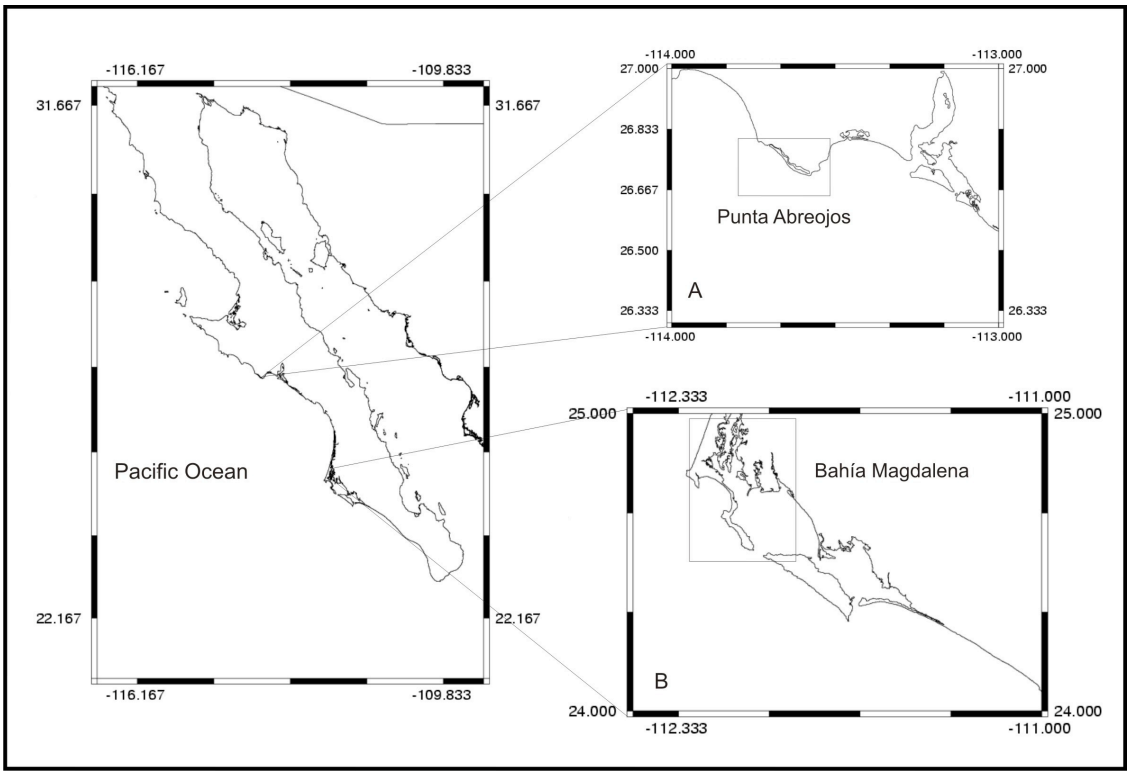

Image courtesy of Labrada-Martagón (2010a)

Figure 24: Baja California, Mexico, with insets for the two field sites with sufficient data, Punta Abreojos (PAO) and Bahía Magdalena (BMA).

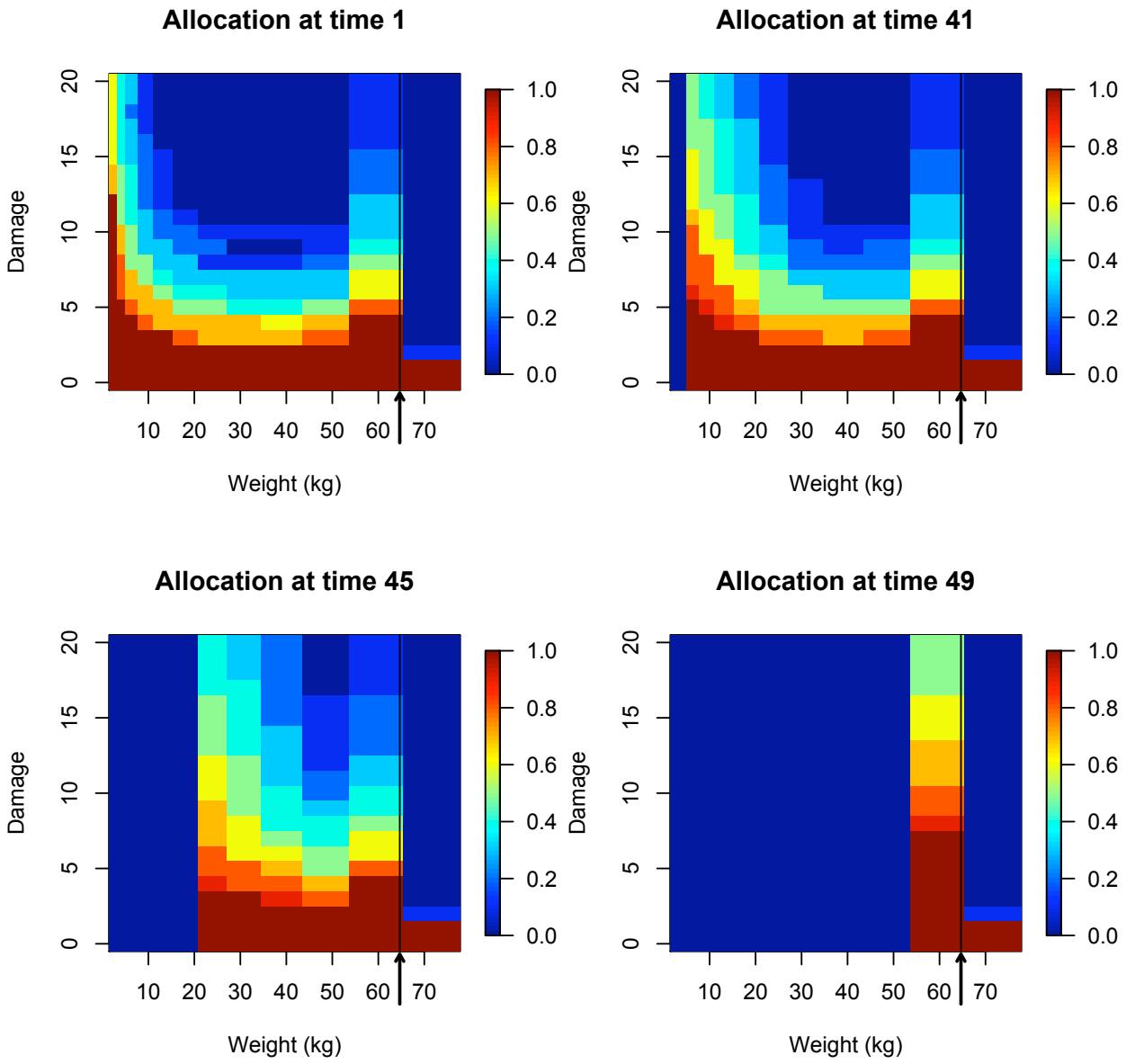

Figure 25: Optimal resource allocation to weight for the PAO region for a given weight and damage level. A value of 1 indicates all resources are allocated to weight, while a value of 0 indicates that no resources are allocated to weight, and thus they go to removing damage. Each panel depicts a different time, where time ranges from 1 to 50. The vertical black line with the arrow below it depicts the weight associated with the length of maturity.

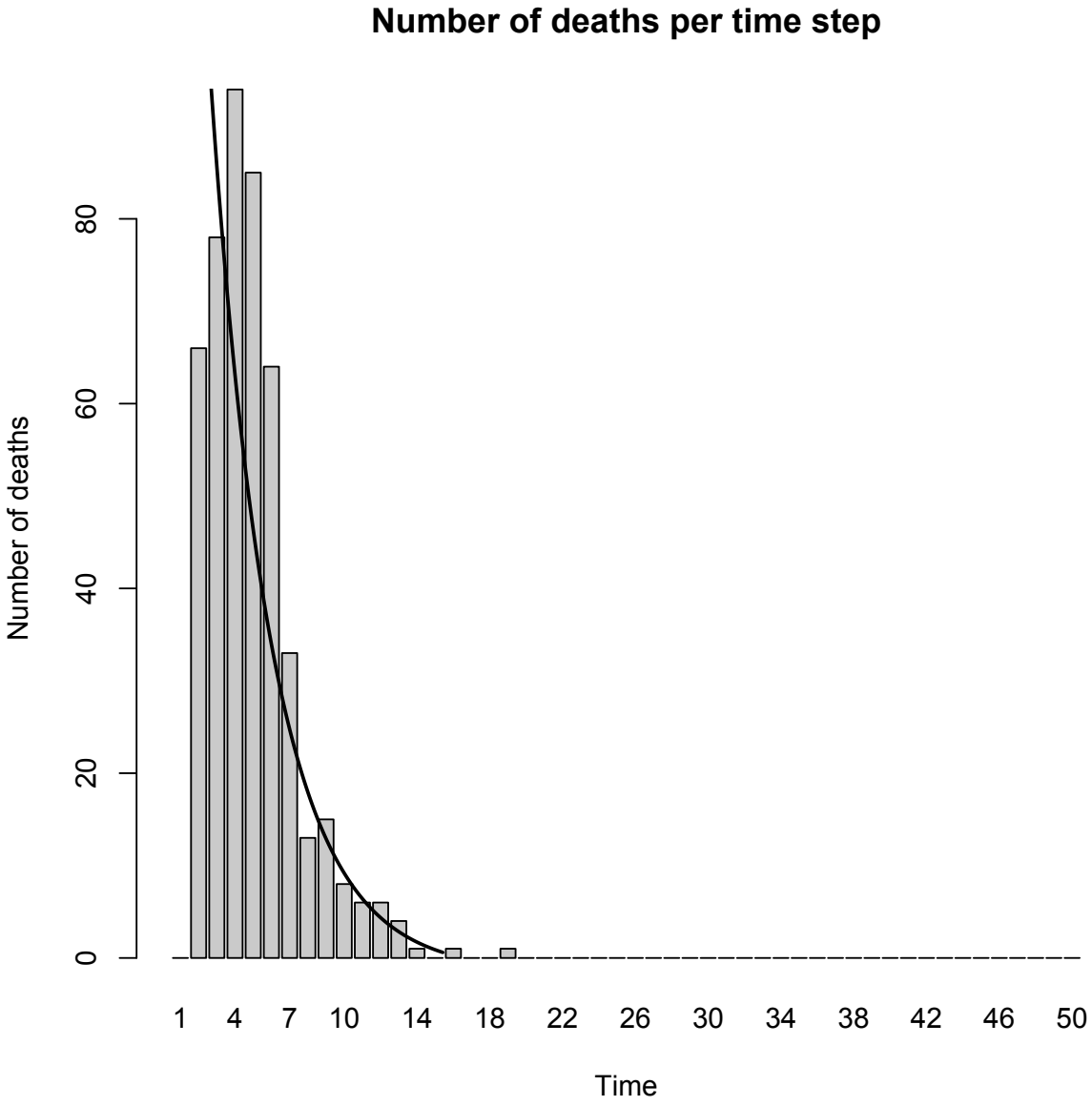

Figure 26: The number of deaths due to mortality at each time step for the forward run of the dynamic state variable model for the PAO region. This distribution roughly follows an exponentially decreasing function (line).

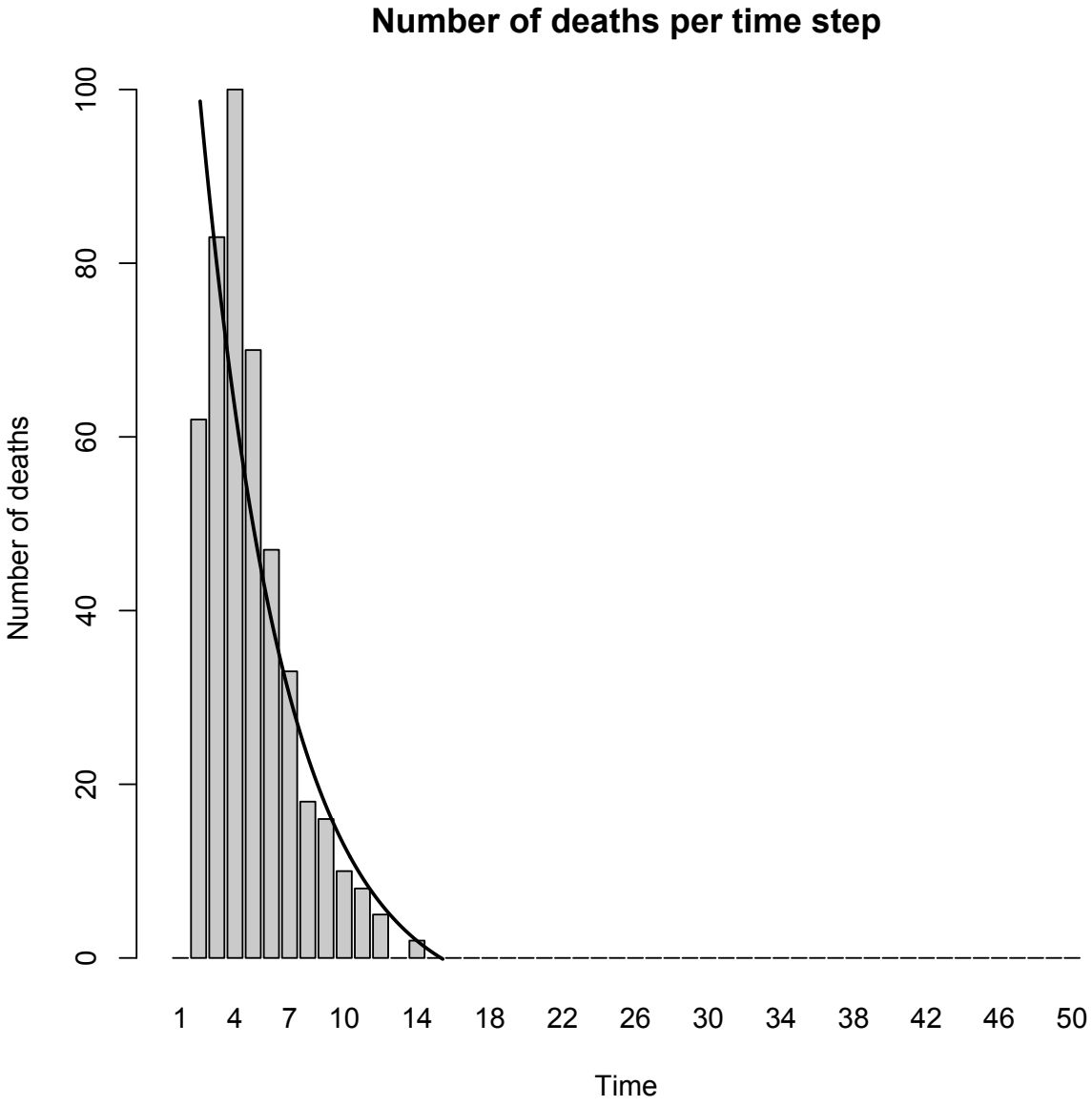

Figure 27: The number of deaths due to mortality at each time step for the forward run of the dynamic state variable model for the BMA region. This distribution roughly follows an exponentially decreasing function (line).

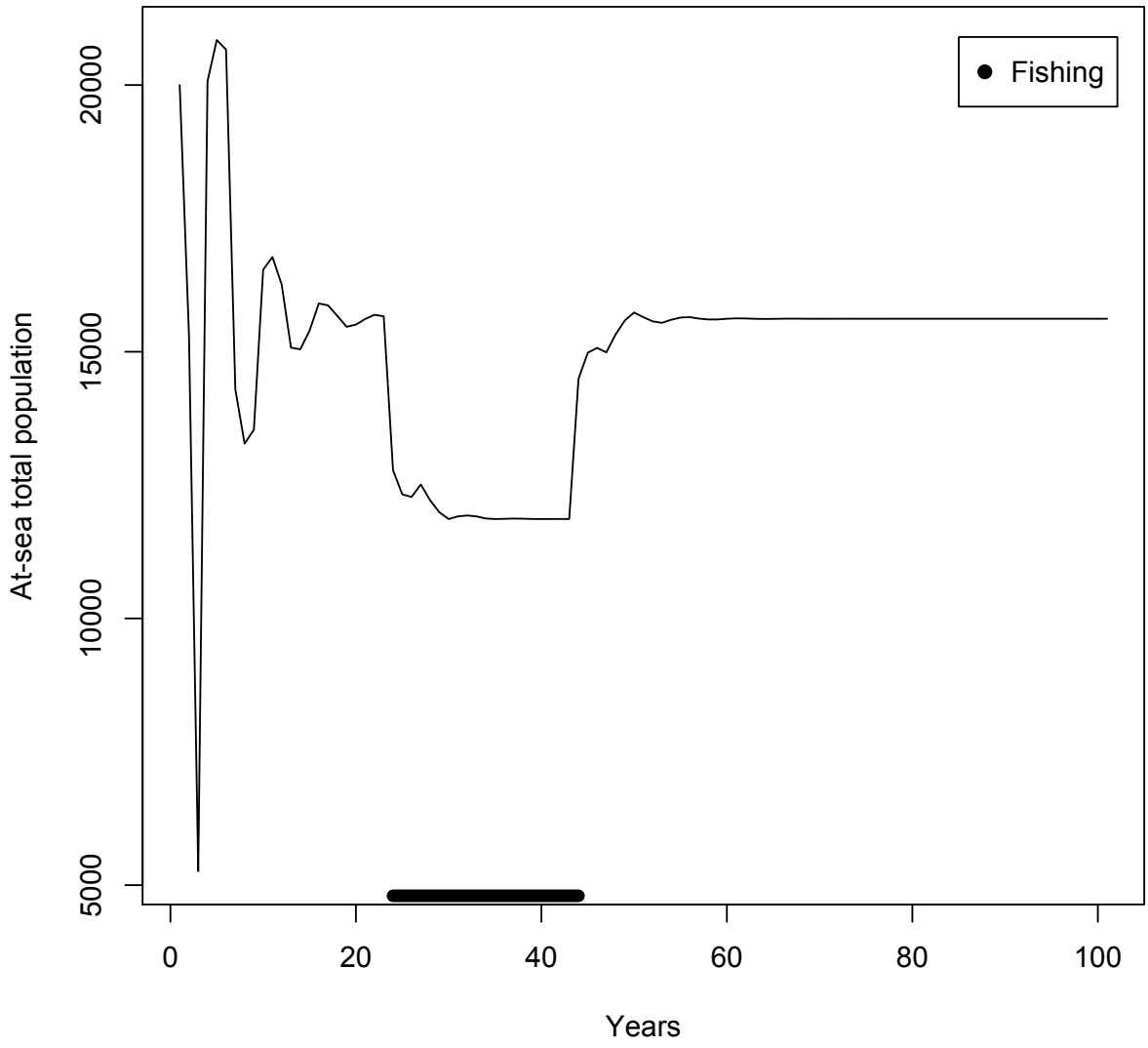

Figure 28: Example of the simulated total at-sea population measured in number of fish, across years, with variable natural mortality case $M^*(3)$. The beginning dynamics depict the population before steady state is reached. Once steady state is achieved fishing is implemented and continues for 20 years (this period is depicted with the black bar along the horizontal axis), after which the population recovers.

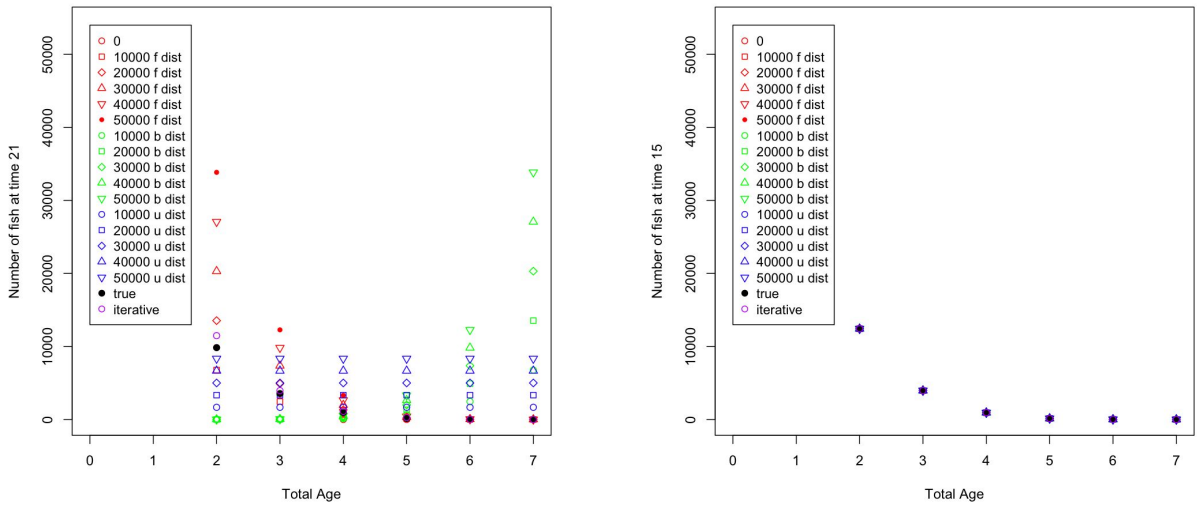

(a) Year 21

(b) Year 15

Figure 29: Using 18 different final conditions, plot of reconstruction values for the number of at-sea fish of each age, over time, for the natural mortality case $M^*(3)$. (a) the final conditions, at time $t = 21$; (b) the results from performing 6 iterations of the reconstruction, at $t = 15$, when all of the values have converged.

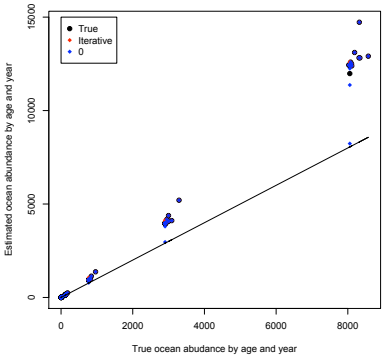

(a) *True*, *Iterative*, and *Zero* final conditions

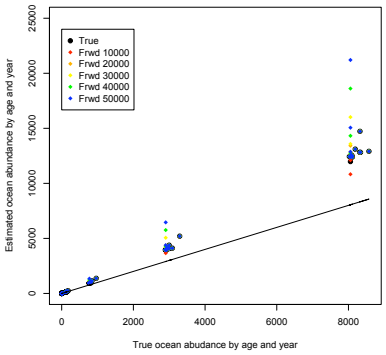

(b) *Forward* final conditions

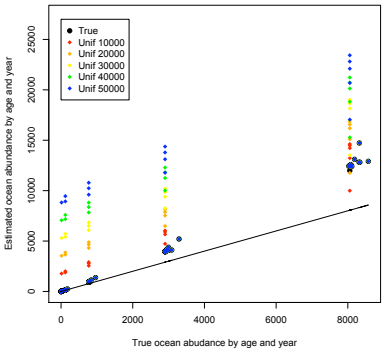

(c) *Uniform* final conditions

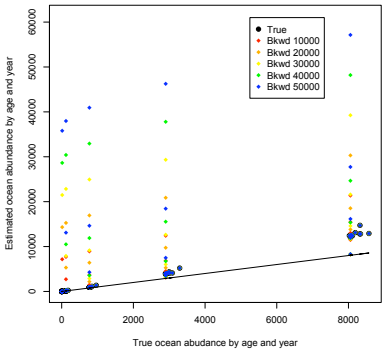

(d) *Backward* final conditions

Figure 30: Plot (a) is the true simulated ocean abundance by age and year plotted against the estimated ocean abundance by corresponding age and year, considering three of the final conditions: *True*, *Zero*, and *Iterative* (see Appendix B). The solid lines in the plots are where the points would lay if the assessment was a perfect match to the simulator. Points which fall above the line correspond to the assessment overestimating the simulated population, those below correspond to an underestimate. Throughout the remaining plots the *True* scenario is repeated for ease of comparison between figures. In plot (b) I have the same points using the *Forward* final conditions. Plot (c) depicts the results for the *Uniform* final conditions. Plot (d) shows the results of the *Backward* final conditions. These results are for the $M^*(3)$ natural mortality scenario, however the other 4 scenarios are qualitatively similar.